The Atomic Nucleus: a Bound System of Interacting Nucleons

K. Heyde
Department of Physics and Astronomy,
Ghent University, Proeftuinstraat 86,
B-9000 Gent, Belgium

(Dated: August 19, 2013)

ABSTRACT

In the present lectures, we discuss how it has become possible to represent the strongly interacting nuclear many-body system of A nucleons in lowest order as nucleons moving independently in an average potential. We start from a description of nucleon forces and how to progress from the early concept of H. Yukawa to up-to-date nucleon-nucleon interactions, describing nucleon scattering data very well. We next discuss the basis structure of the independent-particle model and show how including the residual nucleon-nucleon interactions, first for a few nucleons and progressing to systems with many interacting protons and neutrons, various excitation possibilities arise. These encompass nuclear pairing as well as the appearance of low-lying collective modes of motion. Collective excitations can at present be described starting from self-consistent mean-field theories. In a final section, we present the main ingredients of this approach. Thereby, a link can be made between on one side the motion of single nucleons in an average potential (shell-model picture), including its correlations, and the appearance of intrinsic structures with the ensueing collective excitations which have been originally formulated in a phenomenological way by A. Bohr and B. Mottelson.

Contents

I. A BIT OF HISTORY: THE EARLY PERIOD FROM RUTHERFORED TO THE NOBEL PRIZE WORK ON NUCLEAR STRUCTURE

In the field of nuclear theory, Nobel prizes were rewarded to E.P.J.Wigner, M.Goeppert-Mayer and J.H.D.Jensen for their discoveries concerning a shell structure in the atomic nucleus (Nobel prize in 1963), and, to A.Bohr, B.Mottelson and J.Rainwater for discovering the deep connection between collective motion and single-particle motion in the atomic nucleus (Nobel prize in 1975). It turns out that those two major discoveries, with the original papers dating from 1949, and, 1950-1953, have put their mark on the later work and the evolution of our understanding of atomic nuclei over the last 60 years with as a major theme, trying to reconcile collective motion with individual nucleon motion within a mean field, incorporating residual interactions. In order to do so, nuclear physicists also needed to understand the nucleon-nucleon interaction as originating from free nucleon-nucleon scattering as well as their effective interaction inside the atomic nucleus.

Our knowledge of the atomic nucleus has mainly been driven by ingenious experimental work. The start came with the α-scattering experiments by Rutherford [1] (1911), experiments that set the length scale characteristic for the extension of the atomic nucleus. Since then, a number of key experiments have disclosed the essential degrees of freedom, at the same time giving rise to an increasing theoretical activity that evolved hand in hand with the experimental developments.

Let us consider some of the very early steps. The discovery of the neutron by Chadwick [2](1932) gave rise, within months to the concept of charge symmetry using the Pauli spin matrices and the SU(2) structure proposed by Heisenberg [3]. Experiments providing indications of particular stability for light α-like nuclei were at the origin of an extension to combine isospin and intrinsic spin into the SU(4) Wigner supermultiplet scheme [4], proposing full charge independence of the nucleon-nucleon interaction. The latter scheme was at the origin of a first primitive kind of nuclear shell model, worked out by Feenberg and Philips in 1937 [5], using simple forces with exchange character [3, 6, 7] in the 30's, describing the

binding energies from ^{6}He to ^{16}O. Discoveries following from radioactive decay studies and inspecting the abundances of the stable elements pointed out the extra stability of nuclei that contained a particular number of protons and/or neutrons at 50, 82 and 126, configurations that posed serious problems to the early shell model. In 1934, Fermi succeeded to perform nuclear reactions using neutrons, in particular slow ones, thereby covering almost all of the then known stable nuclei (Fermi *et al.* [8]) and extended the experimental knowledge on atomic nuclei in a major way. These results resulted in the concept of a compound nucleus, resulting from the strong interactions between protons and neutrons [9] which allowed a description of neutron cross-sections as well as the statistical characteristics at high excitation energy in the nucleus. These concepts resulted in a new picture of the atomic nucleus to be considered as a charged liquid drop (by Bethe and Bacher [10] and von Weizsäcker [11] in the mid 30's) and was at the origin of a theoretical description of the phenomenon of nuclear fission, presented by Bohr and Wheeler [12]. On the other hand, the high precision obtained in atomic physics studies of the hyperfine structure in atoms gave results on magnetic dipole moments and electric quadrupole moments by Schmidt and Schüler [13, 14] that pointed towards independent particle motion characterizing the odd nucleon in odd-A nuclei and the presence of an electric quadrupole charge distribution for the nucleus (as shown by Casimir [15]). A systematic study of quadrupole moments by Townes *et al.*, in 1949 [16], was inconsistent with a single nucleon moving in a central potential indicating the need of an induced deformation.

By the end of 1940, it was clear that the experimental data were pointing towards two almost contradictory facets of the atomic nucleus: independent particle motion vs. collective structure. In the field of nuclear theory, Nobel prizes were awarded to M. Goepert-Mayer and J. Hans D. Jensen "for their discoveries concerning nuclear shell studies" [17, 18] and to A. Bohr, B. Mottelson and J. Rainwater "for the discovery of the connection between collective motion and particle motion in atomic nuclei and the development of the theory of the structure of the atomic nucleus based on this connection" [19–21].

It turned out that those two major steps forward, however, resulted in seemingly conflicting views with on one side the individual nucleon motion and on the other side collective degrees of freedom. There have been major developments since on a theoretical understanding of both the shell-model and mean-field methods, intimitely connected through underlying symmetries over a period of ~ 60 years. This would have been impossible without the enormous developments of experimental methods for both the acceleration and detection of particles and nuclei, first starting from stable nuclei, later moving away from stability with the extensive use of radioactive beams.

II. INTRODUCTION

Before attempting to start a description of the atomic nucleus as a bound system of interacting nucleons, it is paramount to learn about the nature of the nucleon-nucleon interactions. We start from the basic properties of nucleon-nucleon interactions as manifested from free nucleon-nucleon scattering. After a short reminder of the Schrödinger equation describing scattering of two nucleons through a central potential V(r), we show that the properties of nucleon-nucleon scattering can be described by a set of nuclear phase shifts. We discuss these results for the dominant scattering channels and their importance in understanding the nucleon-nucleon interaction as a function of the collision energy in free space. The next step is to derive an analytical form describing the experimental scattering data. We are able to constrain the most general form using general invariance properties from quantum mechanics which the nucleon-nucleon interaction should obey. We stress in particular the importance of a tensor term, which is related to the Yukawa picture using one-pion exchange as one of the decisive elements describing nucleon-nucleon forces, as well as the need of a spin-orbit term. We present an example of one of the early realistic nucleon-nucleon forces

(meaning the force is able to describe nuclear phase shifts up to $E_{lab} \sim 400$ MeV) as well as the more recent Argonne potentials. These nucleon-nucleon forces describe the extensive experimental data set of nucleon-nucleon phase shifts extremely well as will be illustrated. Moving to very recent work, it is shown that the most important central components of the free nucleon-nucleon interaction can be derived from lattice QCD calculations.

Attempting to describe the very light nuclei such as ^{3}H and ^{3}He starting from realistic nucleon-nucleon interactions, however, leads to underbound nuclei. This shows the need of introducing three-nucleon interaction terms which is illustrated for the nuclei up to mass number A=12 (^{12}C), indicating the need of both two-nucleon and three-nucleon terms to describe these very light nuclei from ab-initio calculations. We close by facing the problems that arise when trying to use these realistic interactions in order to describe the effective interactions inside the nucleus, containing many interacting protons and neutrons.

The stability of nuclei and abundances of the elements (BE(A) $\sim$ A), as well as early experimental data on nuclear ground-state spins and magnetic moments in many odd-mass nuclei were all pointing towards the existence of a central potential in which nucleons move, to a large extent, as independent particles. In a first part we discuss the concept of an independent-particle model, showing that a harmonic oscillator potential enlarged with a centrifugal $l.l$ and spin-orbit $l.s$ term, is able to describe consistently the proton and neutron numbers corresponding to nuclei with increased stability. We go on showing in some detail the salient features of the shell-model structure (single-particle energy spectra and wave functions, the shell-gaps in the spectra,...).

We then discuss nuclei containing two nucleons outside of a closed-shell system and analyze the energy correction that results from the interaction between these two "valence" nucleons. In order to obtain quantitative results, we start from simple central forces to derive the interaction energy, splitting the degeneracy of the two-nucleon system. A generic property shows up, i.e., the two nucleons (protons or neutrons) preferentially pair up in a state of angular momentum J = 0. We illustrate this important result with examples such as the separation energy of a nucleon from a given nucleus as well as analyzing energy spectra of nuclei with two nucleons outside (or missing) of a closed-shell core.

We move on to make the simple analyses, in which the two nucleons are constrained to one single-particle orbital, more realistic. In general, the two nucleons can occupy more single-particle states and consequently give rise to a number of possible configurations, forming a quantum mechanical basis to solve the nuclear energy eigenvalue problem, starting from a given two-body interaction. We present, in detail, the procedure for a simple nucleus ^{18}O, in which the two valence nucleons can move in the N=2 ($1d_{5/2}$, $2s_{1/2}$, $1d_{3/2}$) orbitals. We discuss the results in the case of ^{18}0 and ^{210}Po, pointing out the presence of a generic pairing results that two-nucleon correlations exhibit throughout the nuclear mass table.

Starting from the detailed discussion for two-nucleon systems, we generalize the nuclear energy eigenvalue problem to systems with a large number of active protons and/or neutrons moving in a given model space (configuration space). To do so we discuss (i) how to build a basis needed to expand the full wave function, emphasizing the rapid increase in dimension of the eigenvalue problem and the corresponding computational issues, and, (ii) how to handle the nucleon-nucleon interaction acting inside the atomic nucleus. The latter point needs particular attention since one can (i) start from relatively simple schematic interactions (putting forward an analytical form), (ii) start from the nuclear two-body matrix elements, called the empirical effective interaction, which are used as parameters that are fixed by fitting the calculated observables (energy, lifetimes in γ- and β,..) to a large set of the corresponding nuclear data in a given region of the nuclear mass table, or, (iii) start from a realistic interaction, however, adapting this force for use inside an atomic nucleus constructing the nuclear G-matrix.

We subsequently go through the various steps in order to apply the nuclear shell model for the rather complex systems of many interacting nucleons (encompassing both protons

and/or neutrons). We illustrate the advances that have been made from the early 1p-shell nuclei (1965) towards recent calculations with very big model spaces and many nucleons. In particular we show results for the sd shell and the fp shell. In the latter case, it is shown that structures reminiscent of collective modes of motion (macroscopic) appear. We make a side-step to show what may be the deeper origin of such collective modes resulting from a purely microscopic shell-model approach.

Finally, we consider nuclei with a single closed shell, such as the N=126 isotones and the Sn isotopes. We point out that the characteristic energy spectra resulting from the shell-model calculations can be understood from an unexpected point of view, emphasizing symmetries connected to the formation of nucleon pairs in long series of isotones (isotopes).

III. NUCLEON-NUCLEON FORCES AND VERY LIGHT NUCLEI

Since our basic assumption in using the shell-model to approximate the complicated nuclear many-body problem of A nucleons interacting inside the atomic nucleus is the use of an effective 'in-medium' interaction, we will start by giving some general discussion of those forces used throughout the present lectures.

It is standard to determine a general form by imposing certain symmetry constraints (see further in the text), and the strength of this general form is fitted to experimental data describing free nucleon-nucleon scattering up to $\simeq 350$ MeV laboratory energy [22].

A. The Bare Nucleon-Nucleon Force

The bare nucleon-nucleon force describes the interaction between two free nucleons (see Figure 1). It is understood that the effect of the Coulomb-interaction is treated separately, so we focus entirely on the effect of the strong interaction between the nucleons.

The derivation of the interaction between free nucleons is based on some important assumptions [23]:

- we consider no substructure in the nucleon, and consider nucleons to describe the essential degrees of freedom,
- the A nucleons interact via a potential,
- relativistic effects are negligible,
- only two-body forces are considered.

The first assumption states that the interaction between two nucleons goes via a potential. The potential depends only on those two nucleons, and the dependence on their coordinates can be expressed in the most general way as:

$$V(1,2) = V(\vec{r}_1, \vec{p}_1, \vec{\sigma}_1, \vec{\tau}_1, \vec{r}_2, \vec{p}_2, \vec{\sigma}_2, \vec{\tau}_2), \tag{1}$$

where $\vec{r}_i$ denotes the spatial coordinate of nucleon $i = 1, 2$; $\vec{p}_i$ the momentum; $\vec{\sigma}_i$ the spin, and $\vec{\tau}_i$ the isospin coordinates.

1. Symmetry Properties and General Structure

The potential $V(1,2)$ has to fulfil a number of symmetry properties, imposed by the nature of the strong interaction between free nucleons:

- **hermiticity**

- **invariance under an exchange of the coordinates**

$$V(1,2) = V(2,1). \tag{2}$$

- **translational invariance**

$$V(1,2) = V(\vec{r}, \vec{p}_1, \vec{\sigma}_1, \vec{\tau}_1, \vec{p}_2, \vec{\sigma}_2, \vec{\tau}_2), \tag{3}$$

with $\vec{r} = \vec{r}_1 - \vec{r}_2$ the relative spatial coordinate.

- **Galilean invariance**

$$V(1,2) = V(\vec{r}, \vec{p}, \vec{\sigma}_1, \vec{\tau}_1, \vec{\sigma}_2, \vec{\tau}_2), \tag{4}$$

with $\vec{p} = \frac{1}{2}(\vec{p}_1 - \vec{p}_2)$ the relative momentum.

- **invariance under space reflection (parity conservation)**

$$V(\vec{r}, \vec{p}, \vec{\sigma}_1, \vec{\tau}_1, \vec{\sigma}_2, \vec{\tau}_2) = V(-\vec{r}, -\vec{p}, \vec{\sigma}_1, \vec{\tau}_1, \vec{\sigma}_2, \vec{\tau}_2). \tag{5}$$

- **invariance under time reversal**

$$V(\vec{r}, \vec{p}, \vec{\sigma}_1, \vec{\tau}_1, \vec{\sigma}_2, \vec{\tau}_2) = V(\vec{r}, -\vec{p}, -\vec{\sigma}_1, \vec{\tau}_1, -\vec{\sigma}_2, \vec{\tau}_2). \tag{6}$$

- **rotational invariance in coordinate space**
  Also introducing the orbital angular momentum $\vec{L} = \vec{r} \times \vec{p}$, only terms of the form $\vec{\sigma}_1 \cdot \vec{\sigma}_2$, $(\vec{r} \cdot \vec{\sigma}_1)(\vec{r} \cdot \vec{\sigma}_2)$, $(\vec{p} \cdot \vec{\sigma}_1)(\vec{p} \cdot \vec{\sigma}_2)$, $(\vec{L} \cdot \vec{\sigma}_1)(\vec{L} \cdot \vec{\sigma}_2) + (\vec{L} \cdot \vec{\sigma}_2)(\vec{L} \cdot \vec{\sigma}_1)$ are possible. Multiplication with an arbitrary function of r^2, p^2 and $\vec{L} \cdot \vec{L}$ does not affect this symmetry constraint.

- **rotational invariance in isospin space**
  Only terms of the form:

$$V_0 + V_\tau \vec{\tau}_1 \cdot \vec{\tau}_2, \tag{7}$$

  are allowed.

A more elaborate discussion of the symmetry properties is given by Ring and Schuck [23].

One can make several combinations with good symmetry, but we present those combinations that have been used mainly in order to construct a realistic bare two-body nucleon interaction.

a. Central Force Component The central forces are local forces since they do not depend on the velocity, and contain only scalar products of the major nucleon variables $\vec{\sigma}$ and $\vec{\tau}$:

$$V_C(1,2) = V_0(r) + V_\sigma(r)\vec{\sigma}_1 \cdot \vec{\sigma}_2 + V_\tau(r)\vec{\tau}_1 \cdot \vec{\tau}_2 + V_{\sigma\tau}(r)\vec{\sigma}_1 \cdot \vec{\sigma}_2 \vec{\tau}_1 \cdot \vec{\tau}_2. \tag{8}$$

This form can be rewritten using certain exchange operators. One defines the spin exchange operator $\widehat{P}^\sigma$:

$$\widehat{P}^\sigma = \frac{1}{2}(1 + \vec{\sigma}_1 \cdot \vec{\sigma}_2), \tag{9}$$

and, likewise, the isospin exchange operator $\widehat{P}^\tau$:

$$\widehat{P}^\tau = \frac{1}{2}(1 + \vec{\tau}_1 \cdot \vec{\tau}_2). \tag{10}$$

The expectation value of $\widehat{P}^\sigma$ becomes:

$$\begin{aligned}\langle SM_S|\widehat{P}^\sigma|SM_S\rangle &= \langle SM_S|\frac{1}{2}\left(1+2(\vec{S}^2-\vec{s}_1{}^2-\vec{s}_2{}^2)\right)|SM_S\rangle \\ &= S(S+1)-1 \\ &= \begin{cases} 1 & \text{for } S=1 \\ -1 & \text{for } S=0. \end{cases}\end{aligned} \tag{11}$$

If $\widehat{P}^\sigma$ would act on a two-particle state with spin $S=1$ (spin-triplet state or spin-symmetric state), there is no change of sign for the spin wave function; if it would act on a $S=0$ state (spin-singlet or spin-antisymmetric), it produces an extra minus sign, to be interpreted as the interchange of the individual spin coordinates. Similar relations hold for $\widehat{P}^\tau$. The exchange operator $\widehat{P}^r$ for the spatial coordinate can be defined through the relation:

$$\widehat{P}^r\widehat{P}^\sigma\widehat{P}^\tau = -1, \tag{12}$$

since the wave function has to be antisymmetric under the interchange of all coordinates of particles 1 and 2. Using (12), $\widehat{P}^\tau$ can be rewritten as:

$$\widehat{P}^\tau = -\widehat{P}^r\widehat{P}^\sigma, \tag{13}$$

and the general central force becomes:

$$V_C = V_W(r) + V_M(r)\widehat{P}^r + V_B(r)\widehat{P}^\sigma + V_H(r)\widehat{P}^r\widehat{P}^\sigma. \tag{14}$$

The coefficients of the different terms in (8) and (14) fulfil the following relation:

$$V_W = V_0 - V_\sigma - V_\tau + V_{\sigma\tau}, \text{(Wigner force)} \tag{15}$$

$$V_M = -4V_{\sigma\tau}, \text{(Majorana force)} \tag{16}$$

$$V_B = 2V_\sigma - 2V_{\sigma\tau}, \text{(Bartlett force)} \tag{17}$$

$$V_H = -2V_\tau + 2V_{\sigma\tau}. \text{(Heisenberg force)} \tag{18}$$

Yet another way of writing down the central interaction makes use of projection operators:

$$\widehat{\Pi}^\sigma_s = \frac{1}{2}(1-\widehat{P}^\sigma) \ , \ \widehat{\Pi}^\sigma_t = \frac{1}{2}(1+\widehat{P}^\sigma), \tag{19}$$

$$\widehat{\Pi}^r_o = \frac{1}{2}(1-\widehat{P}^r) \ , \ \widehat{\Pi}^r_e = \frac{1}{2}(1+\widehat{P}^r). \tag{20}$$

Since table I indicates that it is sufficient to know the spin and isospin symmetry in order to establish the correct antisymmetry of the wave function, one can write the central force in terms of the operators ${}^{ij}\widehat{\Pi}$, defined as:

$${}^{ij}\widehat{\Pi} \equiv {}^{(2T+1)(2S+1)}\widehat{\Pi} \equiv {}^{2T+1}\widehat{\Pi}^{2S+1}\widehat{\Pi}, \tag{21}$$

$${}^{2T+1}\widehat{\Pi} = \frac{1}{2}\left[1-(-1)^T\widehat{P}^\tau\right], \tag{22}$$

$${}^{2S+1}\widehat{\Pi} = \frac{1}{2}\left[1-(-1)^S\widehat{P}^\sigma\right]. \tag{23}$$

The expression for the central force then becomes:

$$V_C = V_C(r)\sum_{i,j=\{1,3\}} a_{ij}{}^{ij}\widehat{\Pi}. \tag{24}$$

The relationship between the various representations of the central force is summarized in table II.

TABLE I: Different combinations giving rise to a totally antisymmetric two-body nuclear wave function. The notation $\langle \vec{\sigma}_1 \cdot \vec{\sigma}_2 \rangle$ is a shorthand notation for the expectation value of the operator in a given two-particle state with total spin S: $\langle (\frac{1}{2}\frac{1}{2}) S M_S | \vec{\sigma}_1 \cdot \vec{\sigma}_2 | (\frac{1}{2}\frac{1}{2}) S M_S \rangle$. Likewise, $\langle \vec{\tau}_1 \cdot \vec{\tau}_2 \rangle$ is a shorthand notation for $\langle (\frac{1}{2}\frac{1}{2}) T T_z | \vec{\tau}_1 \cdot \vec{\tau}_2 | (\frac{1}{2}\frac{1}{2}) T T_z \rangle$.

$\langle \vec{\sigma}_1 \cdot \vec{\sigma}_2 \rangle$	$\langle \vec{\tau}_1 \cdot \vec{\tau}_2 \rangle$	S	T	spatial
-3	-3	0	0	odd
-3	1	0	1	even
1	-3	1	0	even
1	1	1	1	odd

TABLE II: Relation between the coefficients of the various representations (equations (8), (14) and (24)) of the central force.

$\langle \vec{\sigma}_1 \cdot \vec{\sigma}_2 \rangle$	$\langle \vec{\tau}_1 \cdot \vec{\tau}_2 \rangle$	$V(\vec{\sigma}_1 \cdot \vec{\sigma}_2, \vec{\tau}_1 \cdot \vec{\tau}_2)$	$V(\widehat{P}^r, \widehat{P}^\sigma)$	$^{ij}\widehat{\Pi}$
1	-3	$V_0 + V_\sigma - 3V_\tau - 3V_{\sigma\tau}$	$V_W + V_M + V_B + V_H$	a_{13}
-3	1	$V_0 - 3V_\sigma + V_\tau - 3V_{\sigma\tau}$	$V_W + V_M - V_B - V_H$	a_{31}
1	1	$V_0 + V_\sigma + V_\tau + V_{\sigma\tau}$	$V_W - V_M + V_B - V_H$	a_{33}
-3	-3	$V_0 - 3V_\sigma - 3V_\tau + 9V_{\sigma\tau}$	$V_W - V_M - V_B + V_H$	a_{11}

b. Two-Body Tensor Force Component The two-body tensor force also has a local character, and has the form:

$$V_T(1,2) = V_T(r)\left(v_{t0} + v_{tt}\vec{\tau}_1 \cdot \vec{\tau}_2\right)\left(\frac{3(\vec{\sigma}_1 \cdot \vec{r})(\vec{\sigma}_2 \cdot \vec{r})}{r^2} - \vec{\sigma}_1 \cdot \vec{\sigma}_2\right) \tag{25}$$

$$V_T(1,2) = V_T(r)\left(v_{t0} + v_{tt}\vec{\tau}_1 \cdot \vec{\tau}_2\right) S_{12}, \tag{26}$$

and S_{12} is the tensor operator defined in expression (25). The tensor force is particularly important since it causes orbital angular momentum mixing. Its presence in the nuclear force is shown by the non-vanishing quadrupole moment of the deuteron, which cannot be proven by a pure central forces alone [23].

c. Two-Body Spin-Orbit Force Component The two-body spin-orbit force has a non-local structure:

$$V_{lS}(1,2) = V_{lS}(r)\vec{l} \cdot \vec{S}, \tag{27}$$

with $\vec{S}$ the total spin of the two-body system, and $\vec{l}$ the relative orbital angular momentum operator for the two-body system. The velocity dependence, or non-local character, enters the expression through the orbital angular momentum.

d. Radial Dependence The radial dependence of the various contributions can be parameterized using simple central potentials. Various forms are often used:

Yukawa potential: $V(r) = -V_0 \frac{e^{-\mu r}}{\mu r}$,

Gaussian potential: $V(r) = -V_0 e^{-r^2/r_0^2}$,

exponential potential: $V(r) = -V_0 e^{-r/r_0}$,

square well: $V(r) = -V_0$ if $r \leq r_0$

$V(r) = 0$ if $r > r_0$.

The strength V_0 and range r_0 are fitted to the experimental data.

The Yukawa potential [24], however, is based on field theory: the long-distance attractive tail of the nuclear force is mediated by the exchange of one pion between the interacting nucleons. The simplest form is derived from the exchange of a single pion. In this case, $1/\mu = \hbar/m_\pi c$ is the Compton wavelength of the pion, and is given by $\mu = 0.70$ fm^{-1}.

Although the effective nucleon-nucleon interaction (active in some limited part of the full Hilbert space and within a nuclear medium) will be largely different from the form of the free nucleon-nucleon interaction [22], we will start considering the properties of the bare force. To a good approximation, and incorporating one-pion exchange (OPEP), this latter force leads to a form of the type [24, 25]:

$$V_\pi^{\rm OPEP} = \frac{1}{3}\frac{f^2}{\hbar c} m_\pi c^2 \Big\{ \vec{\sigma}_1 \cdot \vec{\sigma}_2 + \Big(1 + \frac{3}{\mu r} + \frac{3}{(\mu r)^2}\Big) S_{12} \Big\} \frac{e^{-\mu r}}{\mu r} (\vec{\tau}_1 \cdot \vec{\tau}_2), \tag{28}$$

with c the speed of light, m_π the pion mass, $\mu \equiv \frac{m_\pi c}{\hbar} = 0.70$ fm^{-1} the reduced pion mass, and $\frac{f^2}{\hbar c} = 0.081 \pm 0.002$ the pion-nucleon coupling constant. The factor S_{12}:

$$S_{12} = 3\frac{(\vec{\sigma}_1 \cdot \vec{r})(\vec{\sigma}_2 \cdot \vec{r})}{r^2} - \vec{\sigma}_1 \cdot \vec{\sigma}_2, \tag{29}$$

is the tensor operator. Expression (28) holds typically for a separation distance $r = |\vec{r}_1 - \vec{r}_2| \simeq 1.5$ – 2 fm, but the actual interaction becomes repulsive (in coordinate space) at distances $r \leq 0.5$ fm.

2. Constructing the Bare Nucleon-Nucleon Interaction

Once a general analytical functional form of the two-body potential has been laid out, the parameters of the various contributions have to be determined. One can accomplish this by analyzing the scattering properties in the various two-body nucleon-nucleon systems, as well as the proton-neutron bound state, i.e. the deuteron. Scattering experiments are performed below the pion-production threshold (~ 350 MeV). This guarantees the appropriateness of the non-relativistic approach, and the nucleons involved can be treated as point-like particles (justifying the assumed existence of a potential). (see Figure 1).

The problem of potential scattering between two nucleons can be described by the 2-particle Schrödinger equation

$$[-\frac{\hbar^2}{2m_1}\Delta_1 - \frac{\hbar^2}{2m_1}\Delta_2 + V(1,2)]\psi(1,2) = E\psi(1,2). \tag{30}$$

Separation in the relative and centre-of-mass coordinates is possible, for radial potentials depending on the relative coordinate r only ($\vec{r} = \vec{r}_1 - \vec{r}_2$) and R=1/2($\vec{r}_1 + \vec{r}_2$), leads to the Schrödinger equation

$$[-\frac{\hbar^2}{2m_r}\Delta_r + V(r)]\psi(r) = E\psi(r), \tag{31}$$

An asymptotic solution (with V(r)$\rightarrow$ 0 for short-range potentials) can be written as

$$\psi_k^+(r) = e^{i\vec{k}.\vec{r}} + f(\theta,\phi)\frac{e^{ikr}}{r}, \tag{32}$$

describing the superposition of a plane wave solution and an outgoing spherical wave, describing the scattering process.

The plane wave can be expanded in its different partial waves as

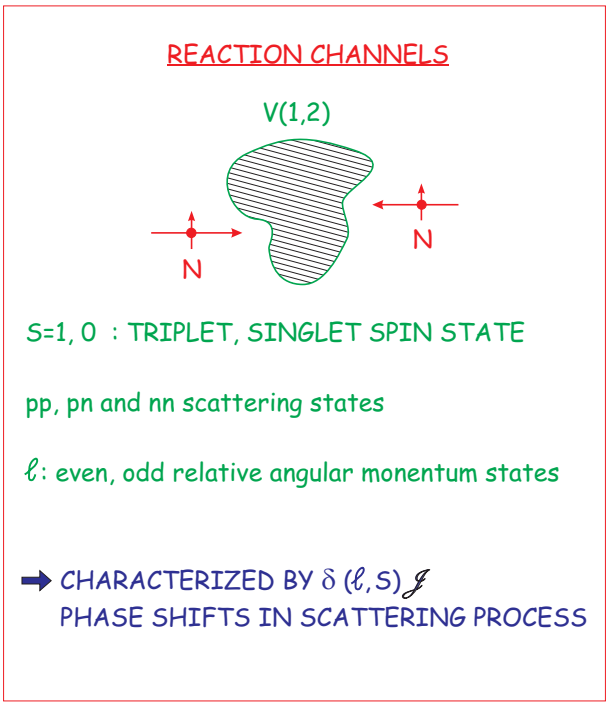

FIG. 1: Scattering free nucleons.

$$\sum_{l=0}^{\infty} i^l (2l+1) j_l(kr) P_l(cos\theta), \tag{33}$$

and the radial form $j_l(kr)$ in the asymptotic region can be expressed as

$$j_l(kr)_{r\to\infty} \propto \frac{1}{kr} sin(kr - l\pi/2) = \frac{i}{2k}[\frac{e^{-i(kr-l\pi/2)} - e^{i(kr-l\pi/2)}}{r}]. \tag{34}$$

In the asymptotic form of the solution $\psi_k^+(r)$, an outgoing spherical wave is present too. Thus, the radial part in each of the partial waves can be expressed as

$$\psi_k^+(r)_{r\to\infty} \propto \frac{i}{2k} e^{-\delta_l(k)} [\frac{e^{-i(kr-l\pi/2)} - S_l(k) e^{i(kr-l\pi/2)}}{r}], \tag{35}$$

with $S_l(k) = e^{2i\delta_l(k)}$.

In the more realistic cases of nucleon-nucleon scattering, the above equations are more complicated because the interaction V(1,2) as described in section II.A will, in general depend on the spin state of the two nucleons which can be in an S=1 or S=0 state and the orientation of the total spin with respect to the relative angular momentum l (expressed by the angular momentum coupling $(\vec{l}, \vec{S})J$) as well as on the charge of the nucleons, i.e., distinguishing nn,pp and np scattering (also expressed by the isospin T quantum number). Because of the presence of the tensor force, which can couple relative angular momenta differing by 2 units, the Schrödinger equations for different values of l, i.e., l=0 and l=2, become coupled. The phase shifts are now given by $\delta(l, S)J(k)$. The general form of the two-nucleon interaction V(1,2) is used to calculate the theoretical phase shifts that are fitted to the experimental data-basis of experimentally deduced phase shifts using a least-squares method, minimizing $\sum_i^n \mid \delta^{th}(l, S)J - \delta^{exp}(l, S)J \mid^2$. These data are given by a set of numbers

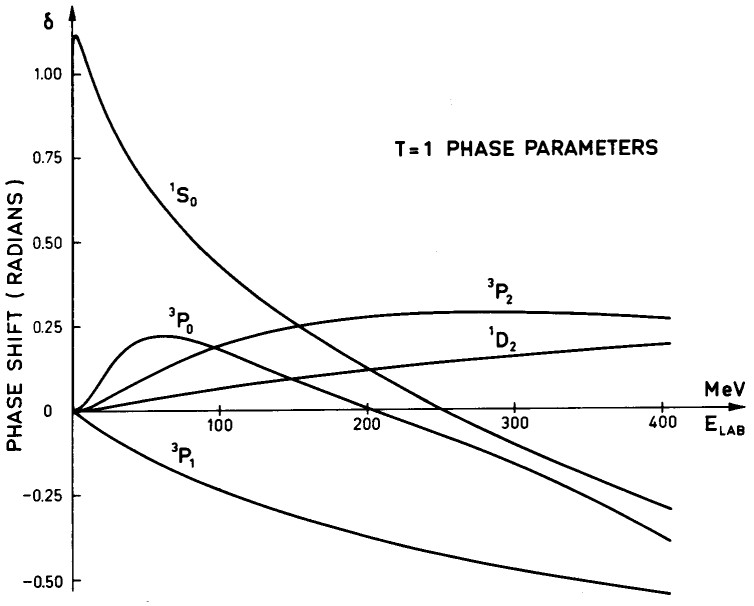

FIG. 2: The nuclear phase parameters for the $T = 1$ channels with $L \leq 2$, up to a laboratory energy of $E_{\rm lab} = 400$ MeV. The phase shifts are given in radians. Positive phase shifts indicate attraction between the nucleons, negative phase shifts repulsion. Figure taken from [25].

(phase shift expressed in radians) as a function of the laboratory scattering energy E_{lab} given in the notation $^{2S+1}l_J$ of which an example is shown in Figure 2 and contain the information about the shape, the strength and the energy dependence of the potential.

There exist a number of potentials that are fitted to nucleon-nucleon scattering data and the deuteron binding energy. Some of the most famous are listed here: the Hamada-Johnston potential (which is presented in Figure 3) [26, 27], the Reid soft-core potential [28], the Tabakin potential [29], the Nijmegen potential [30], the Paris potential [31, 32], the Bonn potential [33, 34], and the modern CD-Bonn, [35], Nijmegen I + II, Reid93 [36] and the Argonne potentials [37, 38].

The Argonne potential consists of 8 (or 18) terms:

$$V_{ij} = \sum_{p=1,8(18)} v_p(r_{ij}) \boldsymbol{O}^p_{ij}, \tag{36}$$

with the operators $\boldsymbol{O}^p_{ij}$ given by:

$$\boldsymbol{O}^p_{ij} = \{\mathbf{1}, \vec{\sigma}_i \cdot \vec{\sigma}_j, \vec{S}_{ij}, \vec{l} \cdot \vec{S}, \ldots\} \otimes \{\mathbf{1}, \vec{\tau}_i \cdot \vec{\tau}_j\}. \tag{37}$$

The potentials have been fitted to 4300 nucleon-nucleon scattering data, and describe the bare scattering process very well over the energy range (up to 350 MeV laboratory scattering energy) [39]. They are phenomenological but describe the essential physics: Coulomb forces, one-pion exchange at the larger nuclear separation distance ($r \simeq 1.5$ – 2 fm), but also the intermediate and short-range parts.

The more data are included, the better the agreement; so it is crucial to fit to proton-proton, neutron-neutron, proton-neutron and deuteron data. Potentials that lack one of these sets in their parameter fit, provide a worse description for that particular set, as demonstrated in [40] for various potential models applied to the proton-proton scattering data.

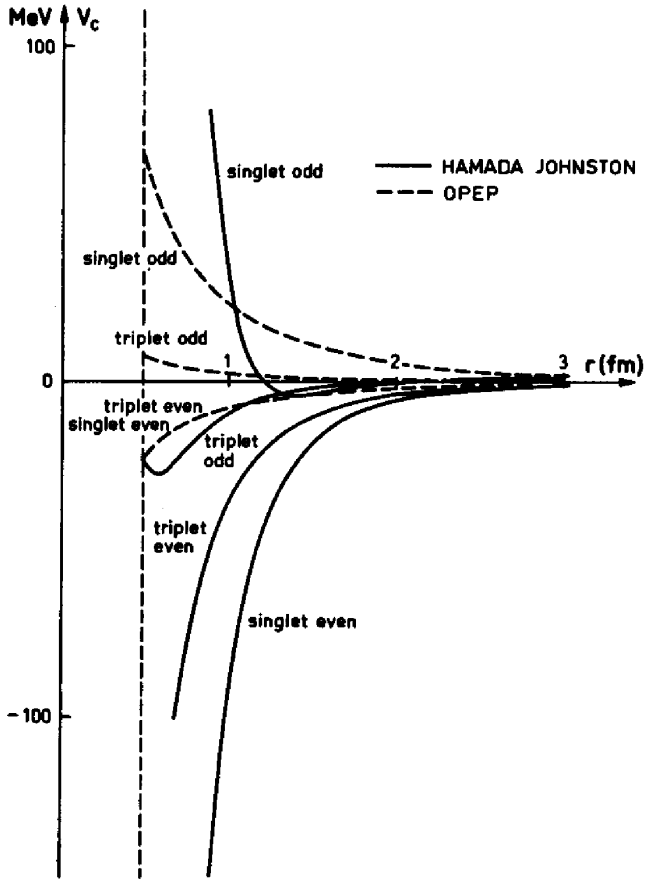

FIG. 3: Phenomenological central nucleon-nucleon potential V_C as obtained from the analysis of Hamada and Johnston [26]. The dotted potentials correspond to the one-pion exchange potential (OPEP) of expression (28). Figure taken from [25].

Even though these potentials provide a precise description of the free nucleon-nucleon scattering, they are still subject to corrections when proceeding towards light nuclei. Usually, the potentials fitted to scattering data tend to underbind light nuclei. The correct binding energy is expected to be found by adding three-nucleon forces [39, 41–44].

An approach different from the ones mentioned above involves writing the nucleon-nucleon potential as a sum over one-boson exchange potentials [45–52].

Moreover, the inclusion of relativistic effects may prove to be important too: given the rather small distance scales, it might be necessary to go beyond the meson picture and to include quark-antiquark pair exchange, as depicted in Figure 4. However, calculations become intractable because of the strong coupling α_s that is too large to allow a perturbative approach [53].

A review on the present understanding of nuclear forces can be found in [54].

B. Ab-initio calculation of very light nuclei

At this point, one may ask the question if one could not start from ab-initio methods and start for the lightest nuclei, using a Hamiltonian containing both 2- and 3-body terms such as

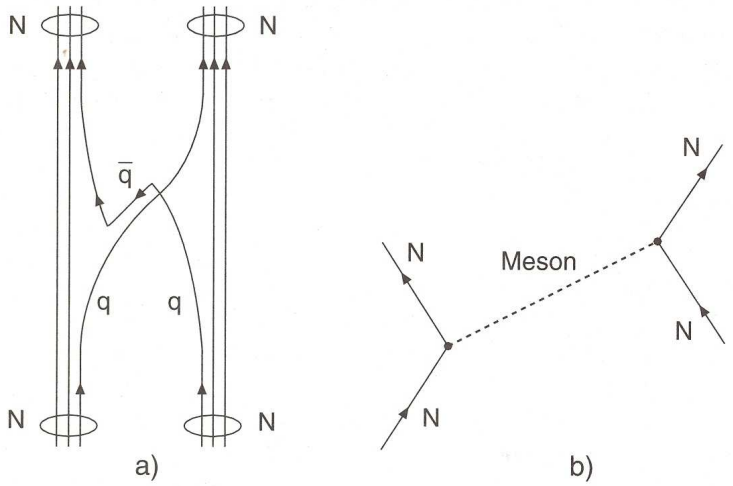

FIG. 4: (a) Representation of quark exchange between nucleons via the exchange of a quark-antiquark pair. Antiquarks are depicted as quarks moving backwards in time. (b) The exchange of a meson is rather similar to this. Figure taken from [53].

$$H = \sum_{i}^{A} T_i + \sum_{i<j} V_{i,j} + \sum_{i<j<k} V_{i,j,k} \quad . \tag{38}$$

Because there is no natural central point in an atomic nucleus, this is a very difficult job and the group of Pandharipande,Carlson,Wiringa,Pieper and co-workers [39, 42–44] has come as far as mass A=12. The two-nucleon interactions used are parametrized through some 60 parameters that fit all known nucleon-nucleon scattering data with a χ^2/data of ≈ 1. In order to go beyond 2-body systems, a 3-body term needs to be included. These are very complex calculations (see Figure 5).

The methods used start from a trial wave function $\Psi_T^{J,\pi}$ that is first constructed for the given nucleus and optimized and contains information about the way nucleons are distributed over the lowest $1s_{1/2}, 1p_{3/2}, 1p_{1/2}$ orbitals. This trial wave function is then used as the starting point for a Green-function Monte-Carlo calculation (GFMC) which projects out the exact lowest energy state with the same quantum numbers by propagating it in imaginary time, or evaluating $\Psi_0 = lim_{\tau\to 0} exp(-(H - E_0)\tau)\Psi(trial)$ [55]. The results are in good agreement with the data, up to A=10.

Also no-core shell-model studies have been carried out recently, moving as far as A=10 and 12 compatible with present-day computer "technology"(see Barrett et al. [56], for more details).

IV. INDEPENDENT-PARTICLE MOTION AND FEW-NUCLEON CORRELATIONS

Nuclear physicists, through many years of investigating atomic nuclei, have been able to find out a lot about the way nucleons are organized inside the nucleus and discovered a number of simple modes of motion using selective experiments. I will remind you of the methods used in extracting this information because, most probably, one will have to copy some of them when exploring unknown territory and we can better learn from the past. The esssential method is very general and can be taken from the first-year textbooks on physics

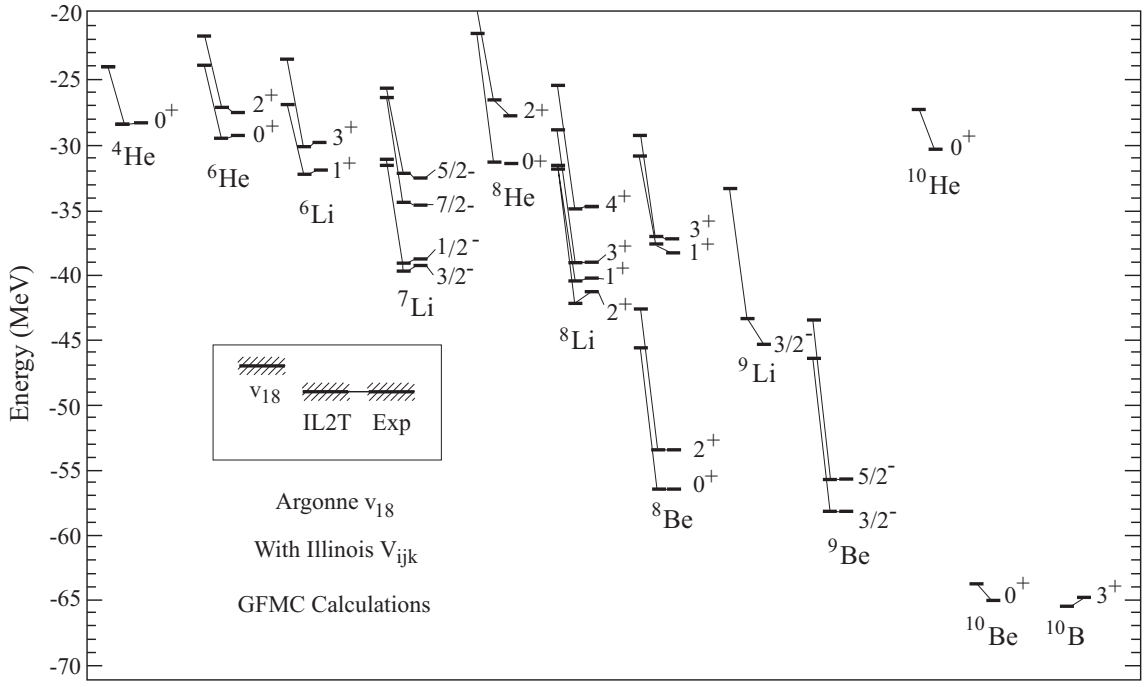

FIG. 5: Energy levels for the light nuclei using a Quantum Monte Carlo (QMC) calculation using 2-and 3-body forces [42].

when studying an oscillator under the influence of an external, time-varying force field. So, whenever we like to find out how something sits together, one can either shake it vigorously and "listen" how the system "responds" or either take it apart into its components. These two avenues have been taken by

(i) studying the response of the atomic nucleus when being probed by external fiels (electromagnetic, weak and strong probes),

(ii) studying the ways in which unstable nuclei decay and emit particles or photons in their way back to stability.

These two principles have been used to disclose some of the essential degrees of freedom that are active inside the nucleus by studying the various "eigen"-frequencies on which the nuclear many-body system resonates (see Figure 6).

In this spirit, besides the discovery of the various decay modes that have given deep insight in the way particles or groups of particles can be emitted from an unstable nucleus, a number of external probes have been used extensively [57].

a. Scattering experiments using electrons, protons, α-particles, ... gave rise to the notion of an average charge and mass field with a profile that resembles very well a liquid drop of charged matter. Moreover, using those probes in ingenious ways, one has been able to map out the motion of nucleons in well-defined single-particle orbitals, much like in a Bohr atom, even studying the velocity distribution of nucleons moving inside the atomic nucleus and thereby learning on the effective nucleon-nucleon forces that act at the very short length scale of nucleon separation.

b. Nuclear reactions in which one, or more nucleons are transferred into a nucleus or taken out of a nucleus: so-called transfer reactions. Those reactions have unambigously

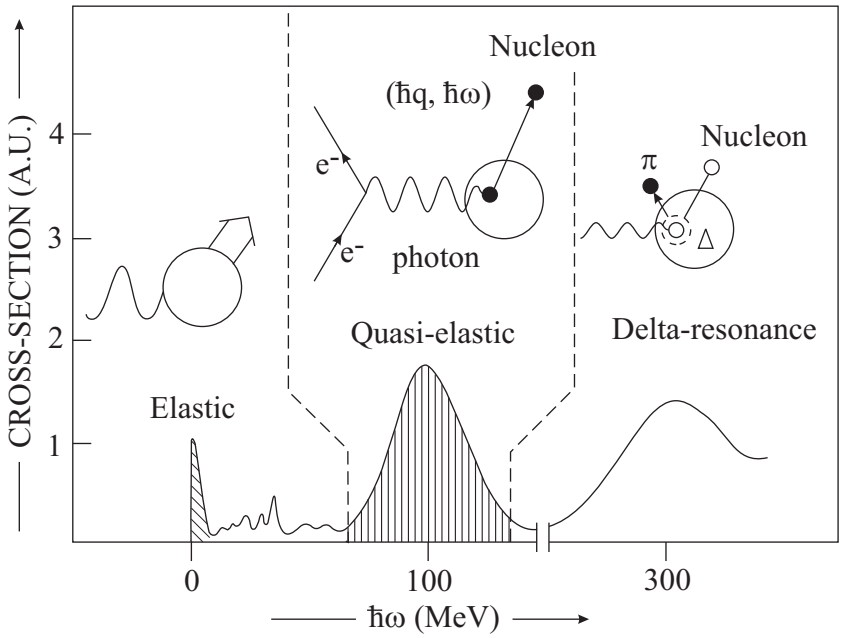

FIG. 6: Schematic cross-section for electron scattering off a nucleus as a function of the energy transfer $\hbar\omega$ (in MeV). Different energy regions are highlighted [57].

shown the organization of nucleons to move in shell-model orbitals in which nucleons like to combine into pairs, much like electrons do in the superconducting state in solid-state physics. This effect has been most clearly shown studying the mass dependence of proton and/or neutron separation energies throughout the nuclear mass table as well as from the energy spacing between the 0^+ ground-state and the first excited 2^+ state in even-even nuclei.

c. Using the disturbance created by a rapidly moving charged particle (or nucleus) when passing the atomic nucleus. The nucleus becomes excited and the internal charge and magnetic structure can be probed in fine detail. Such reactions showed, e.g., the quadrupole reduced transition probabilities for heavy nuclei. These data are a direct measure of the coherence between individual nucleons moving inside the atomic nucleus and present a most interesting variation with mass number A. So one notices that the nucleus can sustain various collective modes, much like a charged drop can vibrate in various modes, rotate,..

d. External probing can also be done using heavy nuclei that come to grazing with a target nucleus to which a fragment may be transferred but also a lot of angular momentum. In this way, the behavior of very regular bands could be formed up to high spin and excitation energy. Data taken within the early experiments showed the existence of superdeformed rotational motion in ^{152}Dy as discoverd in 1986 by Twin and co-workers [58]. The extensive use of state-of-the-art gamma-arrays in recent years has given rise to detailed mapping of nuclear excited properties at very high rotation frequencies.

The essential point here is that ingenious experimentation using - for each time span, of course - the best and most advanced accelerators, detection techniques and analyzing methods, the nucleus has provided us with surprises and challenges.

All these experimental data, derived from the limited region of the nuclear mass table, the region where a variety of observables could be measured, have led us to - let us call it - a

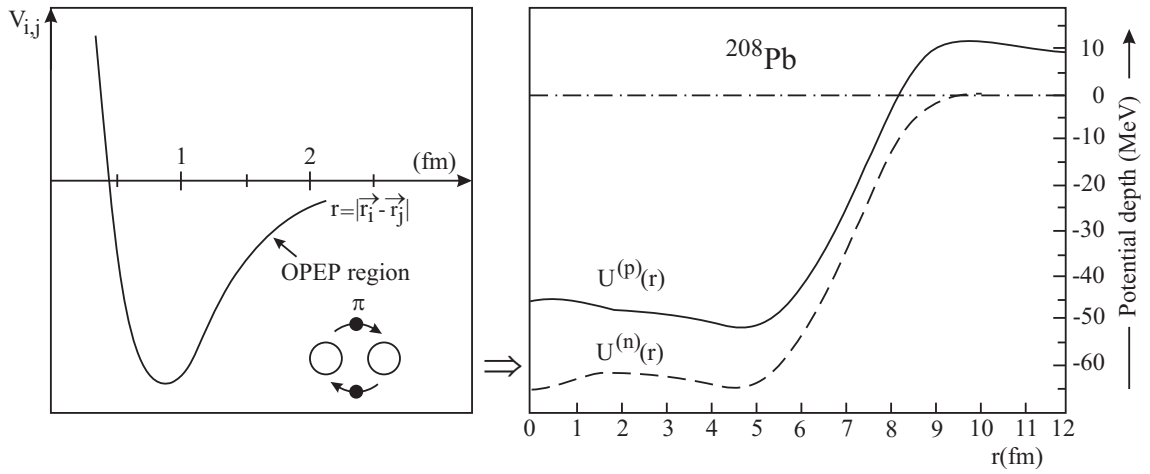

FIG. 7: Schematic picture of the free nucleon-nucleon interaction (left-hand side) and average potentials $U^{(p)}(r)$ and $U^{(n)}(r)$ derived using Hartree-Fock methods and an effective Skyrme force (right-hand side) [57].

"canonical" picture of the atomic nucleus. These results emerged from investigations by a lot of people, in trying to reach deep understanding of how protons and nucleons are organized and make up atomic nuclei: Heisenberg [59], Wigner [60] who applied concepts of symmetries to spin and spin-isopin degrees of freedom, Mayer [61], Haxel, Suess and Jensen [62] devising the independent particle shell-model, Bohr and Mottelson [63], explaining collective effects in atomic nuclei as elementary modes, Elliott [64, 65], bridging the gap between the nuclear shell-model and the collective structures using the SU(3) model,...

The picture showing up is one in which the n-n force generates an average field (Figure 7) in which, quite naturally for every such system, a well-ordered set of single-particle orbits emerges. The residual effects, caused by the nucleon-nucleon correlations, have to be treated subsequently (using more advanced shell-model methods, using the dynamics of the liquid-drop model, using mean-field HF(B) approaches,..) and we show that various collective modes of motion could originate.

A. Independent particle model

Our starting point is the use of a simplified central potential (harmonic oscillator, square-well potential) and study the solution to the motion of a nucleon (proton,neutron) in such a potential. The one-body Schrödinger equation

$$(\frac{\hat{p}^2}{2m} + U(r))\varphi(\vec{r},\vec{s}) = \varepsilon\varphi(\vec{r},\vec{s}), \tag{39}$$

leads to the standard solution of the type

$$\varphi_{n,l,m_l,m_s}(\vec{r},\vec{s}) = R_{n,l}(r)Y_l^{m_l}(\theta,\varphi)\chi_{1/2}^{m_s}(s). \tag{40}$$

It is interesting to express the single-particle solution in an angular momentum coupled representation (changing from the (l,s) basis to the (l,s)j coupled basis) through the relation

$$\psi_{(n,l,1/2)j,m}(\vec{r},\vec{s}) = R_{n,l}\sum_{m_l,m_s}\langle l,m_l 1/2 m_s \mid jm\rangle Y_l^{m_l}(\theta,\varphi)\chi_{1/2}^{m_s}(s), \tag{41}$$

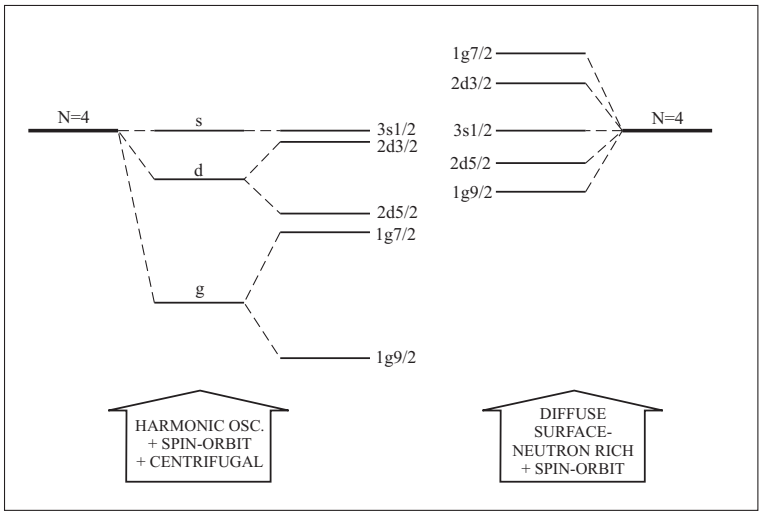

FIG. 8: Single-particle splitting of the N=4 h.o. energy levels (left part) adding the quadratic orbital and spin-orbit coupling and (right part) adding only the spin-orbit splitting perturbation)

in which now l,s=1/2,j and m are the good quantum numbers to specify the single-particle state. Using the harmonic oscillator potential, this leads to the energy eigenvalues (N+3/2)$\hbar\omega$, with N=2(n-1)+l. This energy spectrum with highly degenerate N major shells does not at all correspond to the experimental observed single-particle energy spectra, except for the stable configurations at 2,8 and 20. It was the addition of a strong spin-orbit interaction term $\zeta(r)\vec{l}.\vec{s}$ as introduced by Mayer and Jensen [61, 62] that gave rise to a splitting of the j= $l \pm 1/2$ degeneracy, coming in line with the experimental observations (see the illustration of the N=4 major shell, when also a term $\xi\vec{l}^2$ is added to the potential in Figure 8). See also [66], Sect.3.1.1 to 3.1.3 for a more technical outline and detailed comparison with experimental single-particle spectra.

When discussing in the remaining part of the lectures the wave function in the (l,s)j coupled basis, we shall specify the wave function as $\psi_{j_a,m_a}(i)$ with j_a a shorthand notation for all good quantum numbers needed to specify the single-particle state uniquely, i.e., $j_a \equiv n_a(l_a, 1/2)j_a$, and i is shorthand notation for the coordinates of the i-the particle, i.e., i $\equiv \vec{r}_i, \vec{s}_i$.

In Figure 9, a general single-particle energy spectrum is shown for both the proton and neutron states.

Exercise: Derive the energy splitting for both the spin-orbit and quadratic orbital perturbations within the (l,s)j angular momentum coupled single-particle basis. Discuss the effect of the sign of these perturbations and its deeper meaning.

B. Two-nucleon systems

1. Two-nucleon wave functions

If we consider the motion of two nucleons outside of a closed shell configuration (which corresponds to completely filled major oscillator shells, such as, e.g., ^{18}O), containing two

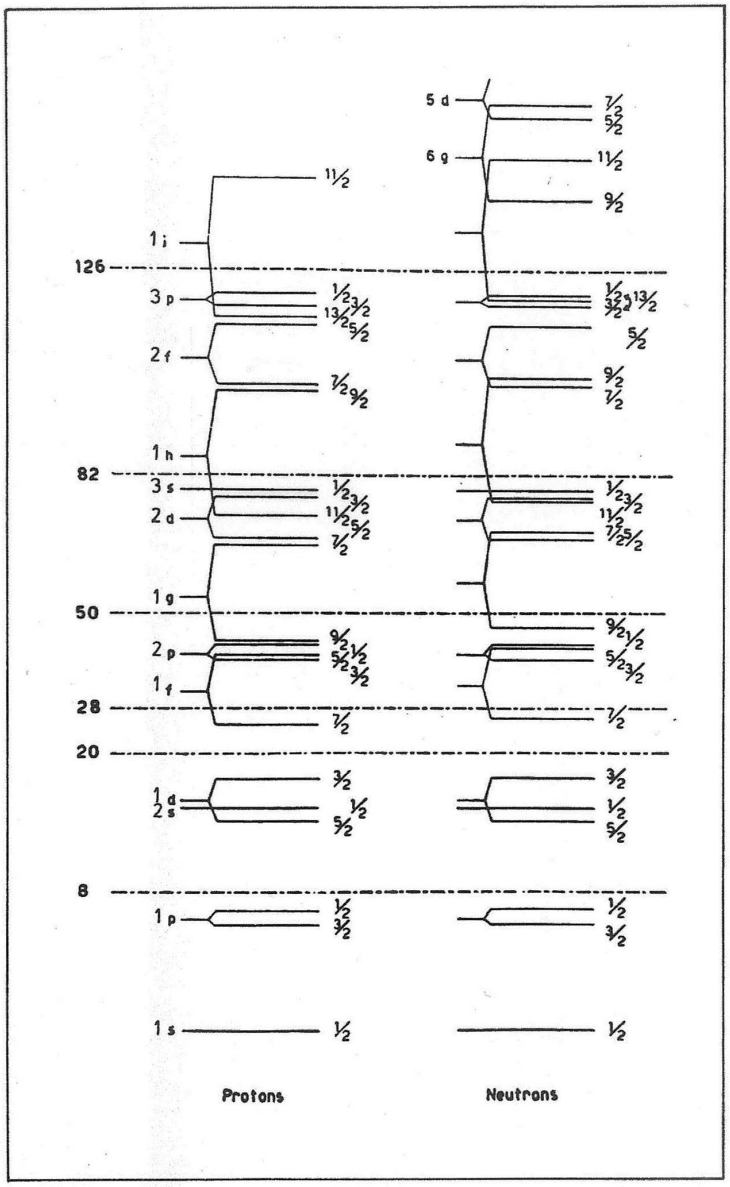

FIG. 9: Single-particle spectra for protons and neutrons

neutrons outside of the closed ^{16}O core, the description of the wave function will result from angular momentum coupling of two identical nucleons (neutrons in the present example), moving in orbitals j_1 and j_2. This results in a two-nucleon wave function

$$\Psi_{j_1 j_2, JM}(1,2) = \sum_{m_1,m_2} \langle j_1 m_1, j_2 m_2 \mid JM \rangle \psi_{j_1 m_1}(1) \psi_{j_2 m_2}(2). \tag{42}$$

The energy of a core nucleus with two identical nucleons moving outside the core is the described by the Hamiltonian

$$\hat{H} = \hat{H}_0 + V(1,2) \equiv \hat{h}_0(1) + \hat{h}_0(2) + V(1,2), \tag{43}$$

in which the independent particle motion of the nucleons, moving separately in the field of

the core, is described by the corresponding single-particle Hamiltonian $\hat{h}_0 = \frac{\hat{p}^2}{2m} + U(r)$. For the remainder we shall use the harmonic oscillator potential $U(r) = \frac{m\omega^2 r^2}{2}$, unless specified explicitely (square-well,Woods-Saxon,.. potential). The residual interaction describing the nucleon-nucleon mutual energy contribution is described by the form V(1,2) (see Sec. III).

The "unperturbed" energy for the two-nucleon configuration (which is the energy when the residual interaction is turned off) becomes

$$\hat{H}_0 \Psi_{j_1 j_2, JM}(1,2) = (\varepsilon_{j_1} + \varepsilon_{j_2}) \Psi_{j_1 j_2, JM}(1,2), \tag{44}$$

whereas the total energy in the two-nucleon configuration (using the Dirac bra-ket notation corresponding to the complex conjugate wave function and the wave function $\langle j_1 j_2 \mid$ and $\mid j_1 j_2 \rangle$, respectively) reads

$$\langle j_1 j_2, JM \mid \hat{H} \mid j_1 j_2, JM \rangle = (\varepsilon_{j_1} + \varepsilon_{j_2}) + \Delta E(j_1 j_2, J), \tag{45}$$

with $\Delta E(j_1 j_2, J)$ the energy correction, lifting the degeneracy of the unperturbed J-states (with $\mid j_1 - j_2 \mid \leq J \leq j_1 + j_2$) given by the two-body matrix element (tbme) $\langle j_1 j_2, JM \mid V(1,2) \mid j_1 j_2, JM \rangle$.

From Lecture I, we have obtained a good idea on how the two-body nucleon-nucleon interaction looks like. Consequently the two-nucleon energy spectrum will depend on this choice and on the specific J value to which the two-nucleon configuration is coupled. Considering at present those situations (with two protons (neutrons) outside of a closed shell or two protons (neutrons) missing from a closed shell (which we call "two-hole" configurations and for which angular momentum coupling holds precisely as for the particle configurations), there is one more important restriction we have to take care of in the construction of the two-nucleon wave function. Because of the indistinguishable nature of identically charged nucleons, we need to impose the condition that the two-nucleon wave function is antisymmetric (a.s.) under the exchange of the coordinates of nucleon "1" and nucleon "2".

This implies the wave function to be written as

$$\Psi_{as}(j_1 j_2, JM) = \sum_{m_1, m_2} \langle j_1 m_1, j_2 m_2 \mid JM \rangle [\psi_{j_1 m_1}(1) \psi_{j_2 m_2}(2) - \psi_{j_1 m_1}(2) \psi_{j_2 m_2}(1)]. \tag{46}$$

Making use of the properties of Clebsch-Gordan coefficients, it is possible to rewrite the above wave function in a form in which the angular momentum of the nucleon with coordinate "1" is coupled to the angular momentum of the nucleon with coordinate "2". Consequently, the wave function becomes

$$\Psi_{as}(j_1 j_2, JM) = \frac{1}{\sqrt{2}} [\Psi_{1,2}(j_1 j_2, JM) - (-1)^{j_1 + j_2 - J} \Psi_{1,2}(j_2 j_1, JM)]. \tag{47}$$

Exercise: Derive this expression using angular momentum recoupling of two independent nucleon angular momenta, as given in Equation (46), in their order of coupling (in the order, 1 with 2 for the two terms).

We call this order 1,2; 1,2,3; 1,2,3,.... the "standard order" for angular momentum coupling which is important to keep track of calculations in a correct way.

In the particular situation that the angular momenta of the two nucleons are identical (and also all other quantum numbers), i.e., $j_1 = j_2 = j$, the two-nucleon antisymmetrized wave function becomes

$$\Psi_{as}(j^2, JM) = \frac{1}{\sqrt{2}} \Psi(j^2, JM)[1 - (-1)^{2j - J}], \tag{48}$$

which is non-vanishing for even J values only. As an example, two nucleons moving in the $1d_{5/2}$ configuration give rise to the $(1d^2_{5/2})$J=0,2 and 4 states whereas the J=1,3,5 states are forbidden by the Pauli principle. For general j value, the result becomes J=0,2,4,...,2j-1. In case $j_1 \neq j_2$, the values of J are bound to the interval $\mid j_1 - j_2 \mid \leq J \leq j_1 + j_2$ and as an example we consider $(1d_{5/2}1d_{3/2})$J, with J=1,2,3 and 4.

2. Two-nucleon correlations: studying the two-body matrix elements

As discussed before, it is the energy correction

$$\Delta E(j_1 j_2, J) =_{as} \langle j_1 j_2, JM \mid V(1,2) \mid j_1 j_2, JM \rangle_{as} (j_1 \neq j_2), \tag{49}$$

which determines the enery spectrum characteristic for a given nucleon-nucleon interaction. Making use of the explicit form of the antisymmetrized two-nucleon wave function, the two-body matrix element (tbme) separates into two terms which are called the "direct" and the "exchange" terms giving the result

$$\Delta E(j_1 j_2, J) = \langle j_1 j_2, JM \mid V(1,2) \mid j_1 j_2, JM \rangle - (-1)^{j_1+J_2-J} \langle j_1 j_2, JM \mid V(1,2) \mid j_2 j_1, JM \rangle, \tag{50}$$

and becomes in shorthand notation $D(j_1 j_2, j_1 j_2; JM) - (-1)^{j_1+J_2-J} E(j_1 j_2, j_2 j_1; JM)$.

In order to derive the generic properties for the two-nucleon energy spectrum we make use of the specific short-range radial two-nucleon force behavior as described in Section III

Starting from the central character of the radial part of the two-nucleon forces, depicted in the form $V(\mid \vec{r}_1 - \vec{r}_2 \mid)$, making use of standard angular momentum properties (see [66], Chapters 1 and 2), it is possible to expand the two-nucleon interaction into its multipoles, described by the Legendre polynomials $P_k(\cos\theta_{12})$, given the resulting form

$$V(\mid \vec{r}_1 - \vec{r}_2 \mid) = \sum_k^\infty v_k(r_1, r_2) P_k(\cos\theta_{12}), \tag{51}$$

The aim is to express the two-nucleon interaction in a form which is the sum of the multipole terms, which can each be separated into the angular coordinates of the interacting nucleons ($\theta_1, \phi_1, \theta_2, \phi_2$), times a radial structure function $v_k(r_1, r_2)$. This important expression reads

$$V(\mid \vec{r}_1 - \vec{r}_2 \mid) = \sum_k^\infty v_k(r_1, r_2) \frac{4\pi}{2k+1} \mathbf{Y}_k(\hat{r}_1) \bullet \mathbf{Y}_k(\hat{r}_2). \tag{52}$$

This form allows, using tensor reduction rules (see [66], Chapter 2 and Sect.3.2.3 for technical details), the matrix element to be written as a sum (over all multipoles), which is in shorthand notation

$$\Delta E(j_1 j_2, J) = \sum_k f_k F^k - (-1)^{j_1+j_2-J} \sum_k g_k G^k, \tag{53}$$

with F^k, G^k radial integrals (containing the harmonic oscillator wave functions and the radial structure function characterizing a specific two-nucleon interaction) and f_k, g_k, functions that are only dependent on the angular momenta j_1, j_2, k, J (Wigner 6j- symbol,...). In principle, the sum over multipoles extends up to infinity. However, the functions f_k, g_k restrict the sums over k into a finite set of contributions. The expression (53) reduces in the case $j_1 = j_2 = j$ to the simpler form

$$\Delta E(j^2, J) = \sum_k f_k F^k. \tag{54}$$

At this point, one should do a numerical calculation of these sums. However, the particular choice of the short-range character of the two-nucleon interaction as a zero-range delta function form, i.e., $\delta(\vec{r}_1 - \vec{r}_2)$, in which case the radial structure function becomes

$$v_k(r_1, r_2) = \frac{\delta(r_1 - r_2)}{r_1 r_2} \frac{2k+1}{4\pi}, \tag{55}$$

simplifies the above sums considerably. First of all, the radial (Slater) integrals become equal with the result

$$F^k = G^k = \frac{2k+1}{4\pi} \int [R_{n_1,l_1}(r) R_{n_2,l_2}(r) r]^2 dr = (2k+1).F^0, \tag{56}$$

Next, the sum

$$\Delta E(j_1 j_2, J) = \sum_k (2k+1) F^0 (f_k - (-1)^{j_1+j_2-J} g_k), \tag{57}$$

can be carried out in closed form, giving rise to the very important and general form of the two-body matrix element

$$\Delta E(j_1 j_2, J) = F^0 (2j_1+1)(2j_2+1) \langle j_1 1/2, j_2 - 1/2 \mid J0 \rangle^2 \frac{1}{2(2J+1)} (1 + (-1)^{l_1+l_2+J}). \tag{58}$$

The corresponding matrix element for $j_1 = j_2 = j$ then becomes

$$\Delta E(j^2, J) = F^0 \frac{(2j+1)^2}{2(2J+1)} \langle j 1/2, j - 1/2 \mid J0 \rangle^2. \tag{59}$$

In the situation that $j_1 \neq j_2$, the matrix elements vanish in those cases in which $l_1 + l_2 + J$ is an odd integer. This result is relaxed for forces other than the zero-range delta interaction but still much smaller than the ones with even integer values for $l_1 + l_2 + J$.

In figure 10, we show at the extreme right-side the two-nucleon energy spectrum for two identical particles moving in a single-particle orbital characterized by j=11/2. This energy spectrum holds as well for a $\mid 1h^2_{11/2}, JM\rangle$ configuration as for a $\mid 1i^2_{11/2}, JM\rangle$ configuration because the energy expression derived before only exhibits a J-dependence.

Exercise: Is it indeed so that their is no dependence of the matrix elements in expressions (53) and (54) on the radial and orbital quantum numbers?

In this same figure, we show the various multipole contributions in the situation for the $1h_{11/2}$ orbital where the k=0 component gives a shift, independent of J, the k=2 quadrupole component, which is leading to a dependence which appears quadratic in J(J+1), up to the k=10 multipole. What shows up is that for the J=0 configuration, all multipoles contribute in coherent way, whereas for the other J-values there is no such regularity.

It turns out that the major outcome from the above study is the fact that when nucleons are moving outside of closed shells, they tend to form J=0 angular momentum coupled pairs, a characteristic which is also called the "pairing" effect. It is this correlation which makes the nuclear shell model a tractable one, since for a heavy nucleus, essentially all nucleons are paired-off to J=0 and only a few "valence" nucleons will determine the low-energy nuclear

Use schematic nucleon-nucleon interaction: purely central.

$V(|\vec{r}_1 - \vec{r}_2|) = \sum_k v_k(r_1, r_2) P_k(\cos\theta_{12})$ ← multipole expansion.

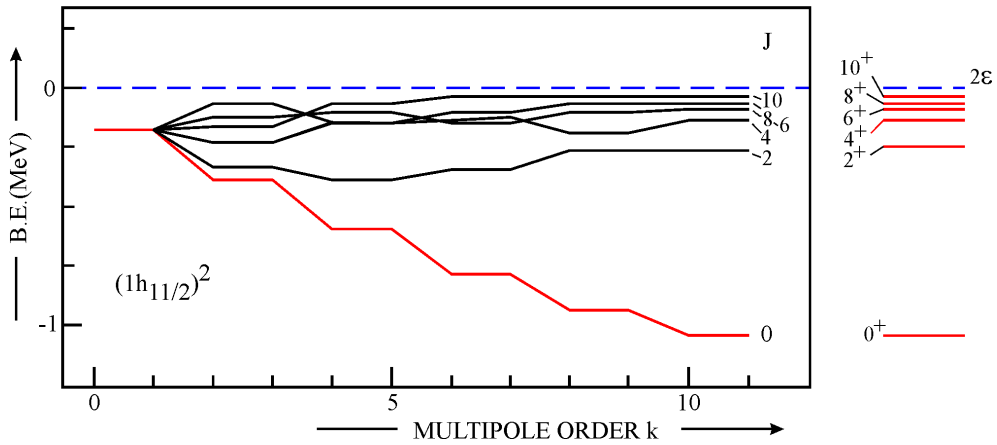

FIG. 10: The k=0,2,...,10 multipole contributions for a two-nucleon system with the nucleons moving in the $1h_{11/2}$ single-particle orbital. At the extreme right, the full energy spectrum is shown, exhibiting a clear separation of the J=0 paired nucleon configuration, with respect to the $J \neq 0$ values of the nuclear spin.

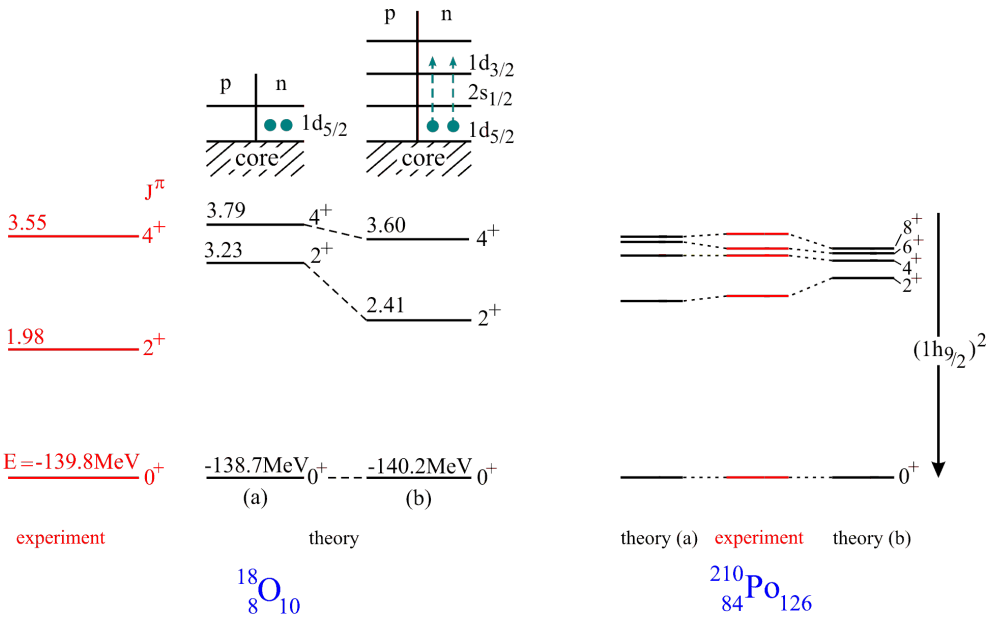

FIG. 11: Energy spectra for ^{18}O (left hand part) and ^{128}Po (right-hand part), respectively. The theoretical spectra in each case, labeled as (a) correspond to the two nucleons moving in the neutron $2d_{5/2}$ and proton $1h_{9/2}$ orbital, respectively. The energy spectra labeled as (b) will be discussed in the next section.

structure properties. We shall discuss this issue later (Lecture III) in more detail and even present an exactly solvable model.

There is an interesting point to be made here with respect to the strength, given by F^0. This implies that there is not a single force "strength" parameter, because the radial integral still exhibits a dependence on the quantum numbers n,l of the orbitals in which the interacting nucleons are moving. We call this a "state" dependence. If however, one uses a specific form of a zero-range interaction, i.e., considering a force which has the form $\delta(\vec{r}_1 - \vec{r}_2).\delta(r_1 - R_0)$, with R_0 the nuclear radius, the Slater integral for two-nucleons moving in orbitals characterized by the quantum numbers $(n_1, l_1, n_2 l_2)$ becomes

$$F^0 = \frac{1}{4\pi}[R_{n_1,l_1}(R_0)^2 R_{n_2,l_2}(R_0)^2](R_0^2). \tag{60}$$

Inspecting the radial wave functions (see Figure 3.8 in [66]), it becomes clear that precisely at the point r=R_0 (at the nuclear radius), the value of the radial wave functions (absolute values) is almost independent of the radial (n) and orbital (l) quantum numbers. This force is also called a Surface Delta Interaction (SDI) (see ref. [22] for more details and examples). In this case, there is an overall interaction strength that describes the two-nucleon energy spectrum.

In the next subsection, we shall give a short discussion on application of these results in various enery spectra.

3. Applications

The method discussed before can in principle be applied to all even-even nuclei having proton and neutron number corresponding to those cases in which we have a core Z_c, N_c (with Z_c, N_c=2,8,20,28,40,50,82,126) and two extra proton or neutron particles (or holes) outside of this core. We have to identify the single-particle orbital that is the dominant one (normally the single-particle orbital that describes the ground-state spin in the corresponding $Z_c, N_c \pm 1$ or $Z_c \pm 1, N_c$ nuclei) in order to derive the corresponding energy spectra.

We show an example for ^{18}O and ^{210}Po, nuclei that are described at the ^{16}O core plus two neutron particles and the ^{126}Pb core plus two protons, respectively (see Figure 11).

Exercise: Using the nuclear data basis of atomic nuclei, compare other situations and evaluate how well the method of considering two nucleons interacting in just a single two-nucleon configuration $\mid j^2, JM\rangle$ is applicable. Also consider, e.g. the even-even Ca nuclei, with Z=20 and N=22,24 and 26 and discuss the corresponding energy spectra.

A beautiful example of the experimental observation of specific two-nucleon correlations, even going beyond the discussion given here is realized in the N=50 isotones considering the Z=42,...48 nuclei (see Figure 12).

C. Configuration mixing and the nuclear eigenvalue problem

It becomes clear that inspecting Figure 11 and comparing the experimental spectrum of ^{18}O with the calculation considering the neutron $2d_{5/2}$ orbital as the most important one, the agreement is not good at all. This implies that we cannot restrict the two neutrons to move only in that orbital but we should consider all possible single-neutron orbitals available beyond the ^{16}O core. Inspecting the energy spectra, we can safely restrict ourselves to the N=2 h.o. shell model orbitals i.e., also consider the $2s_{1/2}$ and $1d_{3/2}$ neutron orbitals. This also implies that in general the correct wave function describing the lowest J=0,2

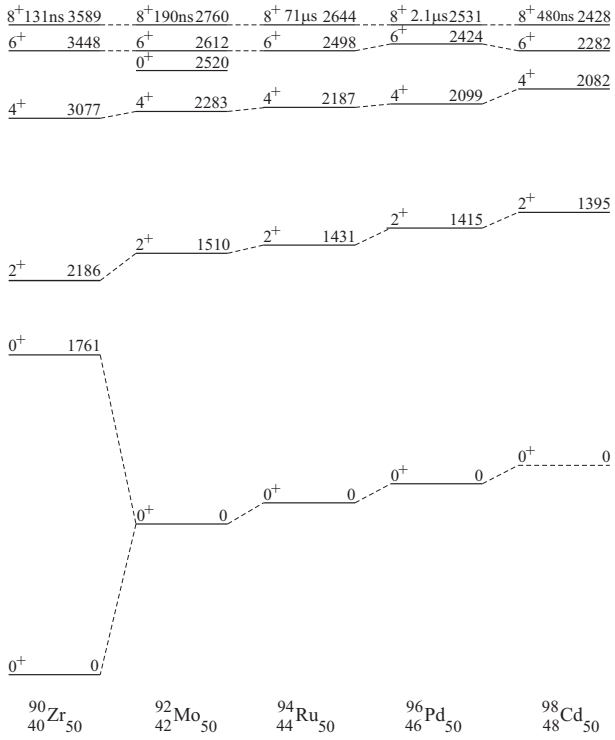

FIG. 12: Energy spectra of the N=50 isotones from Zr(Z=40) up to Cd(Z=48) concentrating on the two-neutron configuration $(1g_{9/2})^{-n}$ in which n describes the numbers of "holes" in this orbital, counting from the Z=50 closed shell. The energy spectra are drawn relative to the highest spin state 8^+.

and 4 spin states should be linear combinations of the basis states. Instead of writing the most general form of the nuclear eigenvalue equation, we shall concentrate to the $J^\pi=0^+$ states. In this case, we have to consider 3 basis configuration, i.e., $\mid \psi_1^0\rangle = \mid (1d_{5/2})^2; 0^+\rangle$, $\mid \psi_2^0\rangle = \mid (2s_{1/2})^2; 0^+\rangle$, and $\mid \psi_3^0\rangle = \mid (1d_{3/2})^2; 0^+\rangle$, respectively.

These basis states are eigenstates of the zero order Hamiltonian $\hat{H}_0 \equiv \hat{h}_0(1) + \hat{h}_0(2)$, but not of the full Hamiltonian, also containing the two-nucleon residual interaction. It becomes clear that the full wave function can be expanded in the above basis as

$$\mid \psi_p\rangle = \sum_{k=1,2,3} a_{kp} \mid \psi_k^0\rangle, \tag{61}$$

with p=1,2,3, describing the three orthogonal linear combinations of the three basis states. This immediately leads to the secular equation, demanding that the state $\mid \psi_p\rangle$ is an eigenstate of the full Hamiltonian $\hat{H} = \hat{H}_0 + V(1,2)$, i.e.,

$$\hat{H} \mid \psi_p\rangle = E_p \mid \psi_p\rangle, \tag{62}$$

or,

$$\sum_k [H_{lk} - E_p \delta_{lk}] a_{kp} = 0. \tag{63}$$

Exercise: Carry out the algebra to derive the secular equation (63), starting from the eigenvalue equation (62).

The matrix (in this case a 3x3 matrix) H_{lk} contains the unperturbed energy of the configurations as well as the corresponding two-nucleon matrix elements, i.e.,

$$H_{lk} = E_k^0 \delta_{lk} + \langle \psi_l^0 \mid V(1,2) \mid \psi_k^0 \rangle, \tag{64}$$

where the "diagonal" energy terms correspond to the unperturbed energies of the three possible cases (in the situation of the 0^+ states these become $\mathrm{E}_1^0 = 2\varepsilon_{1d_{5/2}}$, $\mathrm{E}_2^0 = 2\varepsilon_{2s_{1/2}}$ and $\mathrm{E}_3^0 = 2\varepsilon_{1d_{3/2}}$, respectively), and the interaction matrix elements $V_{lk} \equiv \langle \psi_l^0 \mid V(1,2) \mid \psi_k^0 \rangle$ are given by

$$V_{11} = \langle (1d_{5/2})^2, 0^+ \mid V(1,2) \mid (1d_{5/2})^2, 0^+ \rangle, \tag{65}$$

with V_{22}, V_{33} similar expressions for the diagonal terms.

For the non-diagonal terms, we obtain the expressions

$$V_{12} = \langle (1d_{5/2})^2, 0^+ \mid V(1,2) \mid (2s_{1/2})^2, 0^+ \rangle, \tag{66}$$

and similar expression for all the other non-diagonal terms. Remind that the energy matrix **H** is a real symmetric matrix.

Starting from the secular equation (63), which can be rewritten as

$$\sum_k H_{lk} a_{kp} = E_p a_{lp}, \tag{67}$$

and making use of the orthogonality expression for the eigenstates $\langle \psi_p \mid \psi_{p'} \rangle = \delta_{pp'}$, one obtains the energy eigenvalue equation

$$\sum_{l,k} a_{lp'} H_{lk} a_{kp} = E_p \delta_{pp'}, \tag{68}$$

or, in shorthand notation

$$\tilde{\mathbf{A}}\mathbf{H}\mathbf{A} = E_p \mathbf{1}. \tag{69}$$

This leads for ^{18}O to the diagonalization of a 3x3 matrix for the 0^+ states. It is easy to construct the energy matrices for all other possible spin states if the two neutrons are allowed to be partioned over the three neutron single-particle orbitals.

Exercise: Construct the energy matrices for the 2^+ and 4^+ states.

For the particular case of just two nucleons outside a closed core, the energy matrices to be diagonalized $\hat{\mathbf{H}}$ have a small dimension because there is only a limited amount of basis configurations that determine the dimension of the model space. There exist different algorithms for matrix diagonalization such as the Jacobi method which is used for dimension $d \leq 50$ (see, e.g. Wikipedia for an outline of the method which is straightforward and can easily be implemented at http://en.wikipedia.org/wiki/Jacobi_eigenvalue_algorithm). The Householder method is used for dimensions typically of the order $50 \leq d \leq 200$, and the Lanczos method for $d \leq 200$ up to very big dimension (see [22]). These latter two methods will be mainly used in nuclei with many protons and neutrons interacting outside of a closed core as presented in [67].

Before moving on to Lecture III, we come back to the example of ^{18}O, in which, studying the 0^+ states, the 3x3 energy matrix is such that the third basis state appears at a considerably higher unperturbed energy (the energy of the diagonal element H_{33} with the interaction energy "switched off"). Consequently, we may, to a first approximation, study

the 2x2 submatrix which gives rise to a quadratic equation in the energy eigenvalue E. Defining V $\equiv H_{12} = H_{21}$, the quadratic equation reads

$$(H_{11} - E)(H_{22} - E) - V^2 = 0. \tag{70}$$

The roots become

$$E_{\pm} = \frac{H_{11} + H_{22}}{2} \pm \frac{1}{2}\sqrt{(H_{22} - H_{11})^2 + 4V^2}, \tag{71}$$

and indicate that the energy difference between the two energy eigenvalues becomes $\Delta E = \sqrt{(\Delta H)^2 + 4V^2}$. This difference becomes minimal 2 $\mid V \mid$ if the unperturbed energies of the two states that mix are equal, i.e., for ΔH =0, and asymptotically, for $\mid H_{22} - H_{11} \mid \gg \mid V \mid$, $\Delta E \rightarrow \Delta H$.

Exercise: Show that in a 2-level model, with $H_{11} = E_1^0 + \chi a$ and $H_{22} = E_2^0 - \chi b$, with a,b > 0, the energies E_- and E_+ approach as a function of the variable χ, with a minimal separation at the point where $H_{11} = H_{22}$. Also show that the energy eigenvalues illustrate a "no-crossing" rule. Moreover, show that the eigenvectors at the point of closest approach of the two eigenvalues are equal mixtures of the basis states $\mid \psi_1^0 \rangle$ and $\mid \psi_2^0 \rangle$ but that the lowest (highest) eigenvalue corresponds to the symmetric (antisymmetric)combination of the basis states for an attractive interaction, i.e., V = - $\mid V \mid$.

V. MANY-NUCLEON CORRELATIONS: INTERPLAY OF SHELL-MODEL AND COLLECTIVE EXCITATIONS

In the former Section IV B, starting from the single-particle nuclear wave functions, we discussed in detail how to construct the two-nucleon wave functions for identical nucleons (protons or neutrons) and studied the way in which the remaining two-nucleon interaction is splitting the original degeneracy of the independent-particle model (IPM). We constructed the two-nucleon eigenvalue equation and could already, for a limited number of nuclei, compare the theoretical outcome with the observed energy spectra.

In the present section, we extend the above method so as to allow us to discuss systems with many valence nucleons moving outside closed shells, containing both protons and neutrons. In order to do so, we should understand how to (i) construct a basis for the many-nucleon configurations and, (ii) how to describe the nucleon-nucleon interaction V(1,2) that is effective inside the nuclear medium, in contrast to the nucleon-nucleon interaction describing nucleon-nucleon scattering in "free" space (see Sect. III).

A. Construction of a multi-nucleon basis

1. Angular-momentum coupled basis

Having constructed, starting from the one-nucleon wave functions $\psi_{j_1 m_1}$ the antisymmetrized and normalized two-nucleon wave functions $\Psi_{as}(j_1 j_2, JM)$, there is a straightfoward method using angular momentum techniques to construct 3,4 and higher number of nucleon wave functions corresponding to a given angular momentum J (and magnetic quantum number M). This method becomes quite involved once going beyond 3 nucleons and will not be discussed in its technical details. The process is inductive in the sense that a fully antisymmetric 3-nucleon wave function is described as a sum of products of wave functions that are antisymmetrized in the coordinates of two nucleons only. This reads

$$\Psi(j^3\alpha, JM) = \sum_{J_1}[j^2(J_1)j \mid\}j^3\alpha J]\Psi(j^2(J_1)j, JM), \tag{72}$$

where the sum J_1 goes over all the allowed even-even values and α is an extra quantum number needed to specify a three-nucleon state with angular momentum J uniquely (it can be such that from three nucleons, and more, there are independent ways to couple the individual angular momenta to the total spin J).

This method can be extended from $2 \to 3, 3 \to 4, ..., (n-1) \to n$ in order to construct the fully antisymmetrized wave functions $\Psi(j^n\alpha, JM)$ resulting as

$$\Psi(j^n\alpha, JM) = \sum_{\alpha_1, J_1}[j^{n-1}(\alpha_1 J_1)j \mid\}j^n\alpha J]\Psi(j^{n-1}(\alpha_1 J_1)j, JM). \tag{73}$$

The expansion coefficient [... |}...], are called coeffients of fractional parentage (cfp) because they express how the fully antisymmetrized (notation a.s.) n-nucleon wave function orginates from each of the fully a.s. (n-1)-nucleon wave functions. More technical details are discussed in [66] (Sect. 3.3).

If we extend the system to describe situations in which protons and neutrons are present, such as ^{18}F with a single proton and neutron moving outside of the ^{16}O closed core, we can use the above methods but since protons and neutrons are distinguishable nucleons, the Pauli exclusion principle no longer holds thus the restriction to construct antisymmetrized wave function ceases. It can be interesting to handle the proton and neutron a.s. states corresponding to the nucleon appearing in a "spin up" or "spin down" configuration in an abstract space called *isospin-space*. This means adding an extra quantum number to specify the nucleonic configuration as being in a neutron state $\mid t = 1/2, t_z = +1/2\rangle$ or in a proton state $\mid t = 1/2, t_z = -1/2\rangle$ (or, equivalently by the notation $\zeta^{t_z}_{1/2}(t)$ with $t_z = \pm 1/2$, respectively). Consequently the one-nucleon wave function describing a proton or neutron state becomes

$$\psi_{(n,l,1/2,1/2)j,m,t_z}(\vec{r}, \vec{s}, \vec{t}) = R_{n,l} \sum_{m_l, m_s} \langle l, m_l 1/2 m_s \mid jm\rangle Y_l^{m_l}(\theta, \varphi)\chi^{m_s}_{1/2}(s)\zeta^{t_z}_{1/2}(t). \tag{74}$$

Using angular momentum methods, we can also couple individual nucleon isospin wave functions to a given total isospin T, which in the case of a two-nucleon system results in the eigenvectors $\mid T = 1, T_z = +1\rangle, \mid T = 1, T_z = -1\rangle, \mid T = 1, T_z = 0\rangle, \mid T = 0, T_z = 0\rangle$ for the nn, pp and pn system (in the np system the proton and neutron state can combine in a symmetric or antisymmetric state) (see [66] (Sect. 3.4) for a more detailed discussion).

The isospin quantum number represents a convenient way to construct many-nucleon wave functions and is a very powerful approach in particular when the nuclear Hamiltonian does not break the isospin symmetry (meaning that all NN interactions should be charge independent, which is of course not the case for the electromagnetic interaction affecting the interaction between protons only). However, it is equally well possible to label the wave functions in the way discussed before and label the state as representing it as a proton or neutron state (writing quantum numbers as $\{n_p, l_p, j_p, m_p\}$ for a proton and similar replacing the index p by n, describing a neutron state.

2. m-scheme basis

An efficient way to construct a basis circumventing the involved angular momentum methods as described before starts by identifying the information needed to characterize the nuclear wave function describing the A nucleons constituting the atomic nucleus.

Starting from a shorthand notation to identify a single-particle wave function $\{\alpha_i\} \equiv \{n_i, l_i, j_i, m_i\}$ as $\psi_{\alpha_i}(\vec{r}_i)$ and imposing the condition to construct a wave funtion antisymmetric in the interchange of the coordinates of any pair of nucleons, one obtains the following determinant-type wave function

$$\Psi_\alpha(1,2,...A) \equiv \Psi_{\alpha_1,\alpha_2,..,\alpha_A}(1,2,...A) = \frac{1}{\sqrt{A!}} \sum_P (-1)^P \prod_{i=1}^{i=A} \psi_{\alpha_i}(\vec{r}_i), \tag{75}$$

in which the α_i characterize the quantum numbers of the A occupied states in the atomic nucleus and the sum extends over all possible permutations of the quantum labels, with P even or odd according to the type of permutation. This wave function is antisymmetric by construction as follows from the properties of determinants implying a multiplication by (-1) for the interchange of any two columns (or rows) in the determinant. Thus, the essential information is given by the set of quantum numbers labeling the occupied orbitals. One can show that there exists a one-to-one corresponding between the wave functions in expression (75) and occupation number states, defined as

$$\mid \alpha_1, \alpha_2, ..., \alpha_A\rangle \equiv a^\dagger_{\alpha_A} ... a^\dagger_{\alpha_2} a^\dagger_{\alpha_1} \mid\rangle, \tag{76}$$

in which $\mid \alpha_i\rangle = a^\dagger_{\alpha_i} \mid\rangle$, denotes the creation of a nucleon in an orbital described by the quantum numbers α_i acting on the vacuum state $\mid\rangle$ with no particles present. This formalism is also called the occupation number representation, and is fully equivalent to the wave function representation (including the antisymmetric character) if the operators fullfil the anticommutation relations $\{a^\dagger_{\alpha_i}, a^\dagger_{\alpha_j}\}$ =0, likewise for the corresponding annihilation operators $\{a_{\alpha_i}, a_{\alpha_j}\}$ =0 as well as the relation $\{a^\dagger_{\alpha_i}, a_{\alpha_j}\} = \delta_{\alpha_i,\alpha_j}$.

Because of the fact that this representation is the most economic way of giving information about the occupied orbitals describing a given basis state, moreover incorporating the Pauli principle, this scheme lends itself to numerical studies. We should mention that the wave function described by expression (75) does not have a good total angular momentum J and posseses only a given projection M, i.e., $M = \sum_{i=1}^{i=A} m_{\alpha_i}$ as a good quantum number.

The many-nucleon wave functions thus obtained are eigenfunctions of the energy eigenvalue equation, if we switch of the two-nucleon interaction, and is described by the independent particle Hamiltonian $\hat{H}^0 = \sum_{i=1}^{i=A} \hat{h^0}(i)$

$$\hat{H}^0 \Psi_\alpha(1,2,...A) = E^0_\alpha \Psi_\alpha(1,2,...A), \tag{77}$$

with $E^0_\alpha = \sum_{i=1}^{i=A} \varepsilon_{\alpha_i}$, being the sum of the A single-particle energies.

In practice, one of course has to carry out projection on good angular momentum quantum number J (and if also using the individual isospin labels to characterize the single-particle states, projection on good isospin T).

Exercise: Consider a system of three identical nucleons (protons in our case) that occupy the $1f_{5/2}$ single-particle orbital. The state with the maximum value in this case is M=+9/2 (and also M=-9/2). Construct all possible partitions of the three nucleons over the possible m substates and find out what the possible J values are in the present example

Using the m-scheme, one can quickly evaluate the dimension of the full configuration space if one has a given number of protons n_π and neutrons n_ν distributed over N_π proton, respectively N_ν neutron, orbitals. The value of N_π is given by the sum over all magnetic substates and over all single-particle j_π orbitals, i.e., $\sum_{j_\pi}(2j_\pi+1)$, which is called the model space degeneracy. The result is given by the combination of n nucleons of N orbitals in all possible ways, expressed by the binomial coefficient product $C^{N_\pi}_{n_\pi}.C^{N_\nu}_{n_\nu}$.

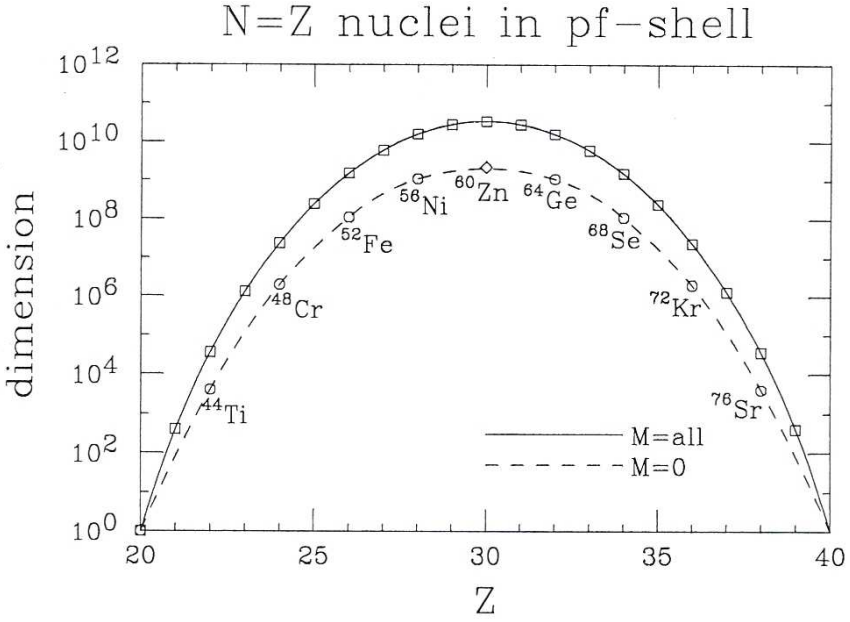

FIG. 13: Complete M-scheme dimension as well as the dimension considering only the M=0 substates for the (fp) shell model space, spanning the mass region starting at ^{40}Ca and ending at ^{80}Zr.

We illustrate the situation in which protons and neutrons are filling the full fp shell (the orbitals situated between N=Z=20 and N=Z=40), in which the degeneracy for protons and neutrons is 20 in each case. It is obvious that the maximal dimension (encompassing all possible M-states) will be maximal at Z=30,N=30 with is the nucleus ^{60}Zn (see Figure 13).

B. Solving the nuclear many-body eigenvalue problem

Having discussed the methods to construct basis states of n valence nucleons moving in a set of single-particle states either in an angular momentum coupled basis J(T), or, using the m-scheme basis, one can construct the corresponding energy eigenvalue equation (or, equivalently, construct the energy matrix $H_{l,k}$). This has already been worked out in Section III studying two nucleon systems as a worked-out example. In the more general case, for a given (Z,N), one first separtes the A nucleons into the ones constituting the "core" (defined by Z_c,N_c) and the valence nucleons which form the model space (with n_π valence protons and n_ν valence neutrons).

Using angular momentum coupling, one has to consider all possible partitions of the valence nucleons (for both n_π and n_ν) over the available proton single-particle orbitals $j_{1,\pi}, j_{2,\pi}, .., j_{k,\pi}$ and likewise for the neutrons, i.e., $j_{1,\nu}, j_{2,\nu}, .., j_{l,\nu}$. This can become rather cumbersome because of the angular momentum coupling at the various stages, e.g. for the proton situation, the basis state becomes

$$\mid \alpha_\pi, J_\pi M_\pi\rangle = \mid [...[(j_1)^{n_1^\pi}_{\alpha_1,J_1}(j_2)^{n_2^\pi}_{\alpha_2,J_2}]J_{12}...(j_k)^{n_k^\pi}_{\alpha_k,J_k}; J_\pi M_\pi\rangle, \tag{78}$$

with $n_\pi = \sum_{i=1}^{k} n_i^\pi$ and similar for the neutron partitioning constructing the neutron basis state $\mid \alpha_\nu, J_\nu M_\nu\rangle$.

Finally, the full proton-neutron coupled configuration space is spanned by the coupled states $\mid \alpha, JM\rangle^0 \equiv \mid \alpha_\pi J_\pi \alpha_\nu J_\nu, JM\rangle$ in which the proton and neutron states are coupled to total spin J. The wave functions for given J, and rank number i $\mid i, JM\rangle = \sum_\alpha c^i_\alpha \mid \alpha, JM\rangle^0$ (here, α is a shorthand notation that labels the basis states uniquely which means that al partitions of valence protons and neutrons over the proton and neutron single-particle states, as described before, are summed over) is the solution of the equation $\hat{H} \mid i, JM\rangle = E(i, J) \mid i, JM\rangle$.

This is equivalent to solving the energy eigenvalue equation

$$\sum_k [H^J_{lk} - E(i, J)\delta_{lk}]a^{(J)}_{ki} = 0. \tag{79}$$

We illustrate the increasing model space for ^{28}Si, containing 6 valence protons and neutrons outside of the ^{16}O core nucleus, starting from the $\mid 1d^6_{5/2}, 0\rangle$ filled proton and neutron configuration (see Figure 14).

C. Effective nucleon-nucleon interactions

The big question now is: what about the nn interaction to be used in constructing the energy matrix. Having discussed about nuclear forces and how we can learn on its basic properties, it looks natural to start from the bare nucleon-nucleon interaction. This, however, poses serious problems because what we need here is the nuclear force acting in the nuclear medium, even restriced to a particular small subspace of the much larger space of all possible configurations.

1. Microscopic effective interactions

The most fundamental way to obtain the nn interaction acting inside the atomic nucleus is to start from the nn interaction as discusssed in Section II, by taking into account the fact that the interacting nucleons are now part of a complex A nucleon system (medium effects, involving the Pauli principle) and the fact that in describing a given nucleus or a given limited model region, one is using a restricted part of the full configuration space. This so-constructed interaction is named an "effective interaction". Here we shall outline only the main steps and for technical details refer to [68–73].

$$\hat{H}\Psi = (\hat{H}^0 + \hat{V})\Psi = E\Psi, \tag{80}$$

where $\hat{H}^0$ is the unperturbed Hamiltonian as described before in Section III. The true wave function Ψ can be expanded in the basis of the solutions to $\hat{H}^0$ as

$$\Psi = \sum_{k=1}^{\infty} a_k \Phi_k, \tag{81}$$

however, in solving for many-body system in practice, only a limited number of configurations is possible, leading to a truncated model space (presence of other nucleons when going from free nucleon-nucleon scattering to in-medium scattering,...) which is called the model space (M). This results in the model wave function

$$\Psi^M = \sum_{k \in M} a_k \Phi_k. \tag{82}$$

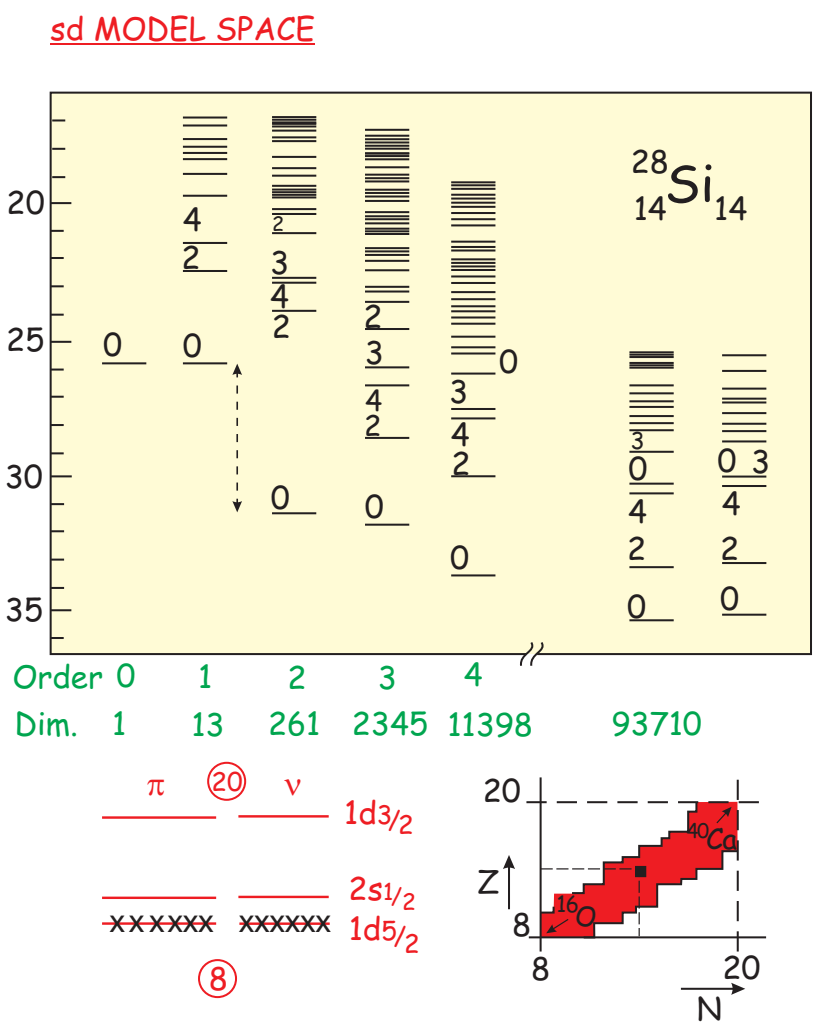

FIG. 14: Model space for, the nucleus ^{28}Si, in which 6 protons and 6 neutrons are partitioned in all possible ways over the full sd model space, starting from a configuration with 6 protons and 6 neutrons filling the $1d_{5/2}$ single-particle orbital.

We should impose, to derive a good truncation scheme , that the lowest M eigenvalues in the complete space be produced exactly in the model space. This implies the definition of an effective interaction $\hat{V}_{eff}$ in the model space defined by imposing the equality

$$\hat{H}_{eff}\Psi^M \equiv (\hat{H}^0 + \hat{V}_{eff})\Psi^M = E\Psi^M. \tag{83}$$

We now define the projection operator $\hat{P}$, with

$$\hat{P} = \sum_{k\in M} \mid \Phi_k\rangle\langle\Phi_k \mid, \tag{84}$$

projecting on the model space and the complementary operator $\hat{Q}$ projecting off the model space (thus $\hat{P}+\hat{Q} = 1, \hat{P}\hat{Q} = 0, \hat{Q}\hat{P} = 0, \hat{P}^2 = \hat{P}$ and $\hat{Q}^2 = \hat{Q}$). These projection operators also have the property that $[\hat{P}, \hat{H}^0]$=$[\hat{Q}, \hat{H}^0]$=0.

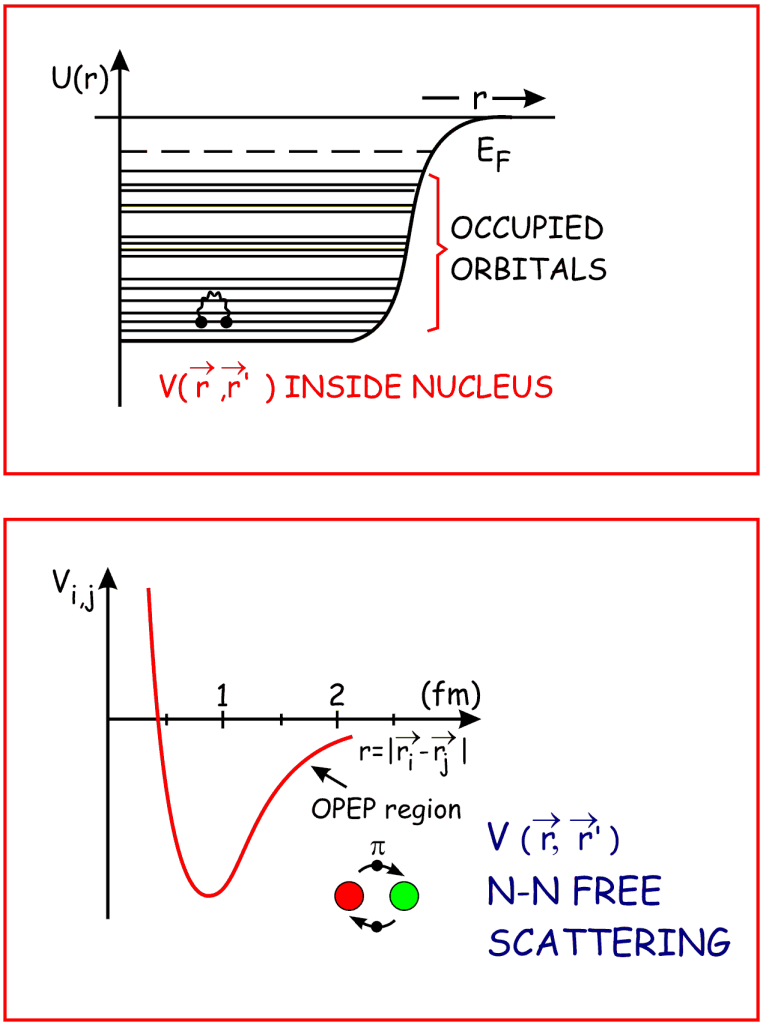

FIG. 15: Schematic figure indicating the step to renormalize the bare nucleon-nucleon interaction (acting in free space) when considering two nucleons interacting inside the atomic nucleus, with all orbitals occupied up to the Fermi level. The Pauli principe only allows scattering to unbound and unfilled bound states.

Starting from the equations $\hat{P}(\hat{H}-E)\Psi=0$ and $\hat{Q}(\hat{H}-E)\Psi=0$, one can express the effective interaction $\hat{V}_{eff}$ as an infinite series, written as

$$\hat{V}_{eff}=\hat{V}+\hat{V}\frac{\hat{Q}}{E-\hat{H}^0}\hat{V}_{eff}. \tag{85}$$

A first step in moving from the bare nucleon-nucleon interaction towards a nucleon-nucleon in medium interaction is one in which all possible final scattering states of the two nucleons inside the nucleus are projected out and can scatter to unoccupied states (unbound states, bound but unoccupied) through acting with the operator $\hat{Q}_{2p}$. This corresponds to sum an infinite class of diagrams, called ladder diagrams, resulting in the Bruecker G-matrix (the in-medium equivalent of the bare nn interaction)

$$\hat{G}(\omega) = \hat{V} + \hat{V}\frac{\hat{Q}_{2p}}{\omega - \hat{H}^0_{2p}}\hat{G}_\omega. \tag{86}$$

This G matrix corresponds to an ineraction which is considerably "softer" as compared with the repulsive short-range behaviour of the bare nucleon-nucleon interaction. This process is illustrated in a schematic way in Figure 15.

The effective interaction, acting now in a reduced model space, e.g., describing the nuclei in the sd shell, can, using the above procedure be constructed this time starting from the so-constructed G-matrix with as a result

$$\hat{V}_{eff} = \hat{G} + \hat{G}\frac{\hat{Q}'}{E_V - \hat{H}^0_V}\hat{V}_{eff}. \tag{87}$$

where E_V is the energy corresponding with the Hamiltonian $\hat{H}^0_V$ for the valence nucleons (defining the model space outside of a closed core) and E_V describing the full energy for the valence space and the projection operator $\hat{Q}'$ is defined such that the ladder diagrams implied by the projection operator $\hat{Q}_{2p}$ are excluded this time.

This full program has been carried out by T.T.S. Kuo and G.E.Brown [74, 75], starting from the bare Hamada-Johnston potential with application first for nuclei near to ^{16}O, and the 1f-2p shells (also called the KB interaction) showing that the effective in-medium effective interaction, starting from the G-matrix and the subsequent very important core-polarization effects, generates a set of two-body matrix elements which describe properties in light nuclei. Similar studies have been carried out for the sd and pf shell, this time starting from meson-theoretical Bonn potentials by M.Hjorth-Jensen et al. [76]. These so-called microscopic effective interactions have been much explored during the last 25-30 years in light up to medium-heavy nuclei.

A major drawback with this approach is the fact that the so constructed microscopic effective forces do not lead to the correct binding energies when considering a long series of isotopes (isotones) in which the number of valence neutrons and/or protons outside of a core nucleus starts increasing. A striking example is the case for the Ca region inspecting the energy gap Δ between the $1f_{7/2}$ and $2p_{3/2}$ orbitals moving from ^{41}Ca to ^{49}Ca [77] filling up the $1f_{7/2}$ orbital with 8 neutrons. The starting value Δ changes from 1.8 MeV to 2.06 only using the KB interaction as compared to the experimental value of 4.81 MeV, a most striking discrepancy. This so-called "monopole" problem has been recognized early on and cured by Pasquini, Poves and Zuker [78, 79] in an empirical way such that the theoretical variation in the single-particle energies fits with the data [80]. This topic on itself would deserve a more detailed discussion to appreciate (i) the problem related to incorrect saturation moving to increasingly heavier nuclei using microscopic effective interactions, (ii) the empirical way to cure this by adjusting mainly the monopole part of the microscopic effective interaction, and, most importantly, (iii) the recognition of the need to incorporate three-body forces in progressing to a consistent description of in medium nuclear forces and the ensuing nuclear structure properties [81]. We also refer to [67] for a discussion on this issue.

2. Phenomenological effective interactions

Opposite to the microscopic approach, the philosophy arose to consider the single-particle energies and the two-body matrix elements as parameters to be fitted to experimental energies through use of the eigenvalue equation in a given restricted model space.

It so appears that the energy matrix elements H_{lk} (see also the discussion in Section III) can be expressed as functions of the most basic elements, i.e., the single-particle energies ε_j

and the two-body matrix elements $\langle j_1 j_2, JM \mid V \mid j_3 j_4, JM\rangle$ specific for the selected model space. In the particular choice of the sd shell, this implies 3 single-particle energies and 63 two-body matrix elements with the protons and neutrons situated in between ^{16}O and ^{40}Ca.

Thus, starting from an initial guess of these "parameters", the energy matrix is constructed, diagonalized and its energy eigenvalues compared with the corresponding experimental data covering a given model space. Then, a least-squares fitting minimizing the quantity $\sum_{i=1}^{N_{data}} \mid E_i^{th} - E_i^{exp} \mid^2$ is carried out. The variation of parameters leads to a set of linear equations resulting in a new set of parameters. The process is iterated until convergence is obtained. More recently, these fits are performed on particularly important linear combinations of matrix elements (for more details see [22]).

The early studies were carried out for the p shell nuclei with 15 tbme (^4He – ^{16}O) by Cohen and Kurath [82]. The sd-region (63 tbme) (^{16}O – ^{40}Ca) was covered by various interactions of the Utrecht group [22, 83, 84] and of Brown, Wildenthal and collaborators [85–87]. Updated USD-A and USD-B interactions have recently been constructed, using an extended data basis in the fitting process [88].

An effective interaction for the full pf-shell (with 195 tbme for the region (^{40}Ca – ^{80}Zr)) model space has been constructed by Honma et al., resulting in the GXPF1-interaction and various adjusted and updated versions [89–91]. This interaction is actually based on a microscopic approach (G-matrix), and further fitted to the experimental data in the mass range $47 \leq A \leq 66$. It gives a good description of nuclei in the mass region $A \simeq 50$. For the lower part of the pf-shell ($A \leq 52$), we already pointed out that the microscopic effective interaction derived by Kuo and Brown, called the KB force [75] shows serious deficiences. Modifications to make it more like a phenomenological interaction have been derived, fitting to various essential date, called the KB1 [78], KB3 (monopole modifications), [79] and KB3G [92] (shell gap adjusted) interactions.

Even higher masses have been studied, going up to the $1f_{5/2}p1g_{9/2}$ model space spanning the region ^{56}Ni – ^{100}Sn [93].

Together with these studies, state-of-the-art computer codes have been developed in order to carry out such large-scale shell-model calculations using the m-scheme basis (ANTOINE [94], OXBASH [95], MSHELL [96], NUSHELL [97], the OSLO code [98], REDSTICK [99], and refer to the code NATHAN [94] and DUPSM [100] for codes using the J(T) basis (see also [67]).

3. Schematic effective interactions

Instead of parameterizing the two-body matrix elements, the option is to make a choice of a more schematic analytic form along the lines as discussed in Section II. Some particular choices of multipole forces, emphasizing the effects of a specific correlation have been made. The low-multipole quadrupole-quadrupole force reads

$$V_{QQ} = \chi(\sqrt{\frac{m\omega}{\hbar}}r_\pi)^2(\sqrt{\frac{m\omega}{\hbar}}r_\nu)^2 \mathbf{Y}_2(\hat{r}_\pi) \bullet \mathbf{Y}_2(\hat{r}_\nu). \tag{88}$$

This force is mainly responsible for describing low-lying quadrupole collective motion (as will be discussed in Sect. V D 1).

Another often used schematic force is the zero-range interaction, which in a more general form can be the radial part of a force that also contains effects related to the two nucleons being in an S=1 (triplet) or S=0(singlet) state and reads

$$V(1,2) = V_0\delta(\vec{r}_1 - \vec{r}_2)(1 + \alpha\vec{\sigma}_1 \bullet \vec{\sigma}_2). \tag{89}$$

Here, there are just two parameters that characterize the interaction, i.e., V_0 and α fixing the strength and the spin exchange character, respectively. It is common then to determine

these parameters in order to reproduce the energy spectra of a few nuclei in restricted model space.

It is also possible to start from even more general analytic expressions, such as a central, a spin-orbit and tensor term (which are also the major terms used to describe the bare nucleon-nucleon ineractions as described before), but this time the parameters specifying the precise form of the interaction are fitted for a larger model space, along the method described when discussing the phenonomenological effective interactions. Such calculations have been performed by Cohen and Kurath [82] (p-shell) and by Richter et al. [101] (fp-shell).

An important interaction is the pairing interaction between identical nucleons (neutrons or protons). In the simplest case, a constant strength is used independent of the single-particle quantum numbers these identical nucleons are moving in. The force is defined such that it gives non-vanishing matrix elements only for $J = 0$ coupled nucleon pairs (see also Sect. V D 2), and with matrix elements given by the expression

$$\langle (j_a)^2, J = 0 \mid V_{pairing} \mid (j_b)^2, J = 0 \rangle = -(-1)^{l_a + l_b} \frac{G}{2} \sqrt{(2j_a + 1)(2j_b + 1)}. \qquad (90)$$

D. Collective excitations in the nuclear shell model

1. *Large-scale shell-model applications*

The possibilities to test the internal consistency and robust characteristics of the nuclear shell model and also test its predictive power have by now been extensively carried out all through the nuclear mass region, except for those regions where the number of protons and neutrons is becoming large and where the full model space leads to intractable large dimensions of the model space (e.g., the deformed rare-earth nuclei in the Z=50-82,N=82-126 mass region). There are by now a number of review papers covering extensively the possibilities and also limitations [67, 102].

The nuclear shell model allows to describe properties of nuclei in the immediate vicinity of closed shells rather well, containing a few valence nucleons, over specific series of isotones (isotopes) even moving away from a closed proton and neutron shell, in particular covering the middle of the sd and pf model spaces. It was known that, even rather near to doubly-closed shell, clear-cut indications for collective (rotational bands) showed up in N=Z nuclei such as ^{20}Ne, ^{24}Mg (sd-shell), ^{48}Cr, (pf-shell) to give just a few examples.

In the following, we concentrate on the ^{48}Cr nucleus (see Figure 16). A full model-space can be handled considering the $(pf)^8$ model space which leads to a full M-space dimension of $\sim 10^7$ basis states. Using a monopole-corrected KB interactions, Caurier et al. [103] have shown that the shell model is generating highly coherent motion between the valence protons and neutrons leading to a rotational behavior for spin up to J=10. Higher up, some strange behavior results, indicating a major change in the underlying configurations describing the band, however, quickly setting back once having passed a "crossing" point (called "backbending"). The experimental observation can be described in a macroscopic approach using concepts deriving from the nucleus being described as a charged, liquid drop amenable to collective oscillations and rotations or the collective model put forward by Bohr, Mottelson and Rainwater [105–107]. It is a very important result that the nuclear shell model, containing a number of interacting protons and neutrons in a large model space, is able to describe these phenomena as a result of the many individual nucleon-nucleon interactions, inducing particular correlations.

Going one step deeper, one can also calculate the electromagnetic decay properties inside this band (the E2 transitions) (see Figure 17). Using those theoretical numbers, and analyzing them using the expressions of the collective model for a pure rotational band, it

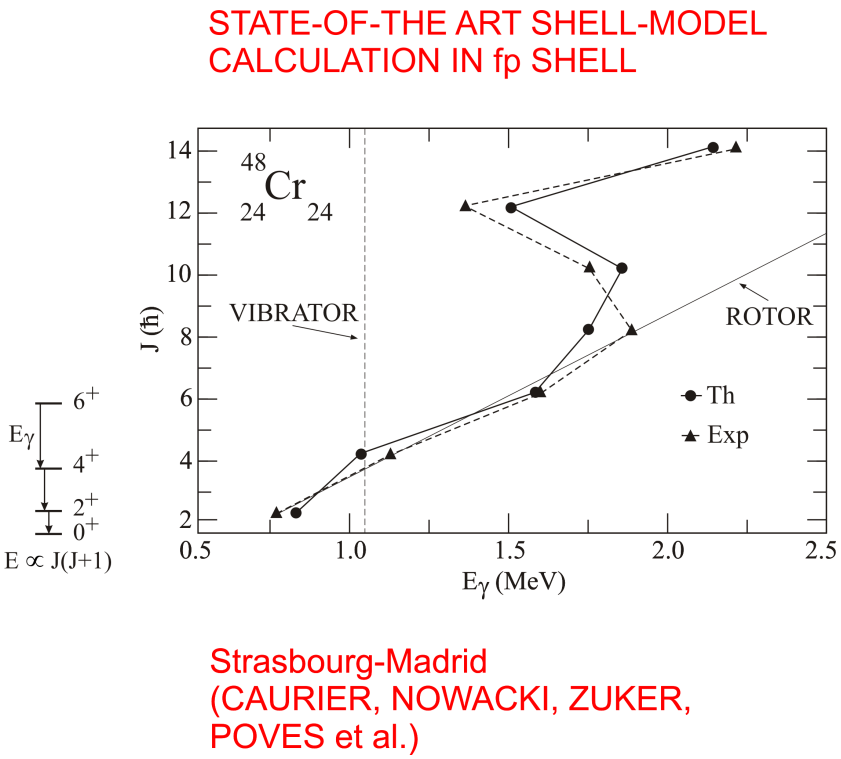

FIG. 16: Energy spectrum for the even-even nucleus ^{48}Cr, comparing with the large-scale shell model spanning the cd RMP-SHAPEcomplete fp shell and with estimates for pure rotor and vibrational spectrum

is most interesting that the nuclear shell model (at least up to spin J=8,10) wave functions are consistend with a single "intrinsic" structure, expressed by the quadrupole moment. Inspecting, however, the comparision between the data, the nuclear shell model and a purely collective model approach, it is most interesing to see that the shell model is doing very well overall. It was shown by Zuker et al. [104] that reducing the huge model space to just the $(1f_{7/2}2p_{3/2})^8$ contains the essential physics and that using this model space, considering a schematic quadrupole interaction, one is able to generate the appearance of rotational collective motion. This opens a deep view on how collective rotational modes of motion and specific shell-model correlated configurations are connected. This connection was first shown in seminal papers by Elliott [64, 65] emphasizing the underlying symmetries in the shell-model wave functions for sd shell nuclei, characterized by the SU(3) dynamical symmetry inherent in a degenerate harmonic oscillator shell model approach, even adding a quadrupole-quadrupole residual interaction. The topic of symmetries could easily take up another lecture.

The road we have taken starting with the IPM, consecutively adding more correlations, has shown that collective effects can be generated in a natural way within the shell model, even opening a road, using the underlying symmetries within the nuclear shell model basis, to come into reach of describing highly correlated modes of nucleon motion.

2. Collective excitations: coherence and symmetries

In our study of the nuclear shell model, we include all possible correlations induced by the effective in-medium interaction. This involves the low multipoles, implying long-range

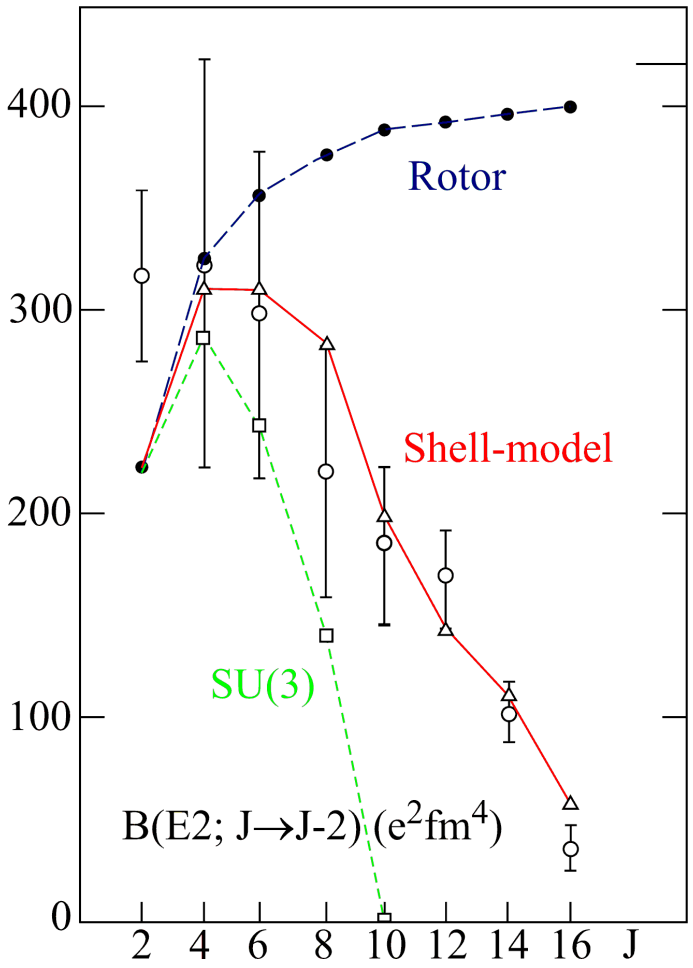

FIG. 17: BE2 values in the even-even nucleus ^{48}Cr ground-state band, comparing with the large-scale shell model spanning the complete fp shell and with the results using a pure K=0 rotational band

correlations extending over the whole nuclear interior. The higher multipoles, on the other hand, are mainly responsible for the almost isotropic scattering of nucleons from a given pair of orbitals (j,m)(j,-m) into any other magnetic substate (j,m')(j,-m') and are at the origin of the pairing gap between the $J^\pi = 0^+$ and the higher spin states. As a consequence of the interplay between the low- and high multipoles present in the effective interactions, a large diversity of energy spectra can very well be described and understood.

We have seen that large-scale shell-model (LSSM) calculations with a number of protons and neutrons outside of closed shells can give rise to rotational bands. This is mainly the result form the quadrupole force acting in the model space, coupling (lj,l+2,j+2) partners particularly strong. On the other hand, we have shown that short-range forces (see Section III) result in a large energy gap separating the 0^+ and 2^+ state when identical nucleons are considered (see, e.g., the examples of ^{18}O, ^{210}Po (Figure 11) and the N=50 isotones (Figure 12)).

It is possible to define a specific interaction that is acting only in the $J^\pi = 0^+$ state resulting from the $(j)^2_J$ configuration. This is obviously not possible using the zero-range interaction because non-vanishing binding energies result for the J $\neq$ 0 states, albeit with quite small binding energies for the highest-spin states. The pairing force, only affecting the

$J^\pi = 0^+$ state, has to be constructed using the occupation number representation.

We define the operator $S_j^\dagger$ acting on an empty shell (reference state called $\mid 0\rangle$) as

$$S_j^\dagger \mid 0\rangle = \mid j^2, J = 0 M = 0\rangle = \frac{1}{\sqrt{\Omega}} \sum_{m>0} (-1)^{j+m} a_{jm}^\dagger a_{j-m}^\dagger \mid 0\rangle, \tag{91}$$

The pairing interaction doing precisely what we intend is then defined as (see [66], Sect. 7.2 for technical details)

$$\hat{H} = -G\Omega S_j^\dagger S_j, \tag{92}$$

and results in the energy spectrum with a binding energy of $E(J = 0) = -G\Omega$ and $E(J \neq 0) = 0$.

If we extend from the 2-particle case to a j-shell filled with n identical nucleons (n even), it is energetically most favorable to put the nucleons in (n/2) pairs, resulting in the "condensate"

$$(S_j^\dagger)^{n/2} \mid 0\rangle, \tag{93}$$

It is now possible to break a pair with J=0 and form two nucleons coupled to angular momentum J. We call this a broken pair state, defined as

$$B_J^\dagger = \sum_m \langle jmj - m \mid J0\rangle a_{jm}^\dagger a_{j-m}^\dagger. \tag{94}$$

This allows us to construct states with an increasing number of broken pairs, up to reaching the mid-shell point $\Omega = j + 1/2$, creating the set of states

$$(S_j^\dagger)^{(n/2)-1} B_J^\dagger \mid 0\rangle, ... \tag{95}$$

This model is an exactly solvable model and carrying out the algebra of it results in the energy spectrum for the (j^n) configurations for identical nucleons given by the expression

$$E(v, n) = -G/4(n - v)(2\Omega_j - n - v + 2) \tag{96}$$

in which the quantum number v (called "seniority") is defined as the number of nucleons that are not coupled in $J^\pi = 0^+$ pairs.

Exercise: Construct the absolute and relative energy spectra for the configuration $(1h_{11/2})^n$ and compare your results with the results we showed in Figure 12 for the N=50 isotones. Also compare with the energy systematics for the even-even Sn (Z=50) nuclei. You will notice that in the Sn nuclei, spanning the region N=50 – N=82, the neutron single-particle energies are more realistic as compared to the schematic model, considering a single j=31/2 shell but still, the basic properties of the schematic model are rather well realized.

The above pairing model has most interesting properties since it can also be solved in an algebraic way, making use of the fact that the operators $S_j^\dagger, S_j$ and their commutator $[S_j, S_j^\dagger]$ are the generators of an SU(2) group (see A. Frank et al. [108] for a detailed discussion).

The pairing model, as applied here to a single-j shell, can be extended for a set of non-degenerate many-j shells, but loses the simplicity of the above exact pairing model, however keeping the essential physics. The Sn region (as is the N=82 and N=126 series of isotones) forms a particularly interesting mass region to test these ideas.

VI. MEAN-FIELD APPROACH

In the mean-field approach, the motion of nucleons as independent (quasi-)particles is derived starting from effective forces and using self-consistent Hartree-Fock (-Bogoliubov) (HF(B)) theory. The effective forces used have been tuned to describe global nuclear properties such as charge radii and ground-state binding energies throughout the nuclear mass surface, encompassing both spherical nuclei, near closed shells [109], and deformed nuclei [110]. Minimizing the Hartree-Fock energy, under the constraint of keeping a number of nuclear multipole moments fixed, can be performed over a range of collective parameters (quadrupole, octupole,...). Most often, this results in a deformed nuclear shape (see Fig 18). Bender *et al.* [111] have recently reviewed self-consistent mean-field models.

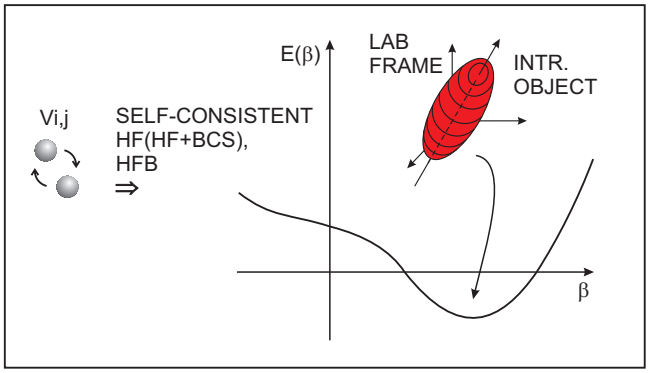

FIG. 18: Illustration of the energy surface E(β) for a single collective parameter (quadrupole deformation, β) which follows from self-consistent Hartree-Fock(-Bogoliubov) calculations.

The main ingredients in the self-consistent mean-field approach encompass the following:

(i) A nucleon-nucleon effective interaction has to be chosen so that the behavior of the nuclear binding energy is well described throughout the whole nuclear mass region, covering spherical nuclei near closed shells as well as deformed nuclei. In recent studies, the interactions used go back to the seminal work of Skyrme [112–114] and Gogny [115–117].

(ii) The single-particle wave functions and the corresponding occupation probabilities are derived self-consistently through a variational method applied to the energy, with the addition of constraints on multipole moments and pairing properties describing the nucleus.

(iii) The nuclear many-body wave function is built from independent (quasi-)particle states.

(iv) Restoration of the symmetries that are broken in the intrinsic frame. This can be performed by projecting the mean-field states onto fixed particle number (N,Z), isospin (T), and angular momentum (J).

The equations describing the mean-field properties are the well-known Hartree-Fock-Bogoliubov (HFB) equations, or an approximate set of HF+BCS equations when a two-step procedure is used in which the particle-hole correlations are considered in the first step (solving the HF equations), and the particle-particle pairing correlations are put in afterwards (solving the BCS equations). From the solutions, one can construct a set of HFB (or HF+BCS) wave functions $\mid \Phi(q)\rangle$ generated in a self-consistent way in which the collective constraining coordinate q acts as a semiclassical parameter (most often quadrupole deformation). As a consequence, the intrinsic state breaks a number of basic symmetries

of the exact many-body states as defined in the laboratory frame. Therefore, one has to restore these broken symmmetries by projecting the mean-field states onto a fixed N, Z, T, J to produce physical states $\mid J, M; q\rangle$ (see Bender *et al.* [111] for technical details).

The operator that projects to a fixed proton (neutron) number is

$$\hat{P}_{N_0} = \frac{1}{2\pi} \int_0^{2\pi} d\phi_N e^{i\phi_N(\hat{N}-N_0)}, \tag{97}$$

whereas the projection operator that selects eigenstates of good angular momentum $\hat{J}^2$ and $\hat{J}_z$ reads

$$\hat{P}^J_{MK} = \frac{2J+1}{16\pi^2} \int_0^{4\pi} d\alpha \int_0^{\pi} d\beta \sin\beta \int_0^{2\pi} d\gamma \mathcal{D}^{*J}_{MK}(R)\hat{R}, \tag{98}$$

where $\hat{R} = e^{-i\alpha\hat{J}_z}.e^{-i\beta\hat{J}_y}.e^{-i\gamma\hat{J}_z}$ is the rotation operator and $\mathcal{D}^{*J}_{MK}$ is a Wigner function.

The correctly projected and normalized states for given spin J and intrinsic projection quantum number K=0 finally looks as follows:

$$\mid JM; q\rangle = \frac{\hat{P}^J_{M0}\hat{P}_{N_0}\hat{P}_{Z_0}}{\langle q \mid \hat{P}^J_{00}\hat{P}_{N_0}\hat{P}_{Z_0} \mid q\rangle^{1/2}} \mid q\rangle. \tag{99}$$

In Fig.19 we illustrate the decomposition of the energy of ^{186}Pb, starting from the (Z=82, N=104) number-projected energy (the small dotted line, also marked with 'Mean-field'), into its various J-components (J=0,2,..,10)(various types of dashed lines). The energies are normalized to the particle-number-projected energy where the minimum appears for the spherical state. Both the prolate (positive $q \equiv \beta_2$ values) and the oblate (negative $q \equiv \beta_2$ values) J-projected energy curves are shown. The energy difference for these J-curves corresponds to the rotational energy of the mean-field states.

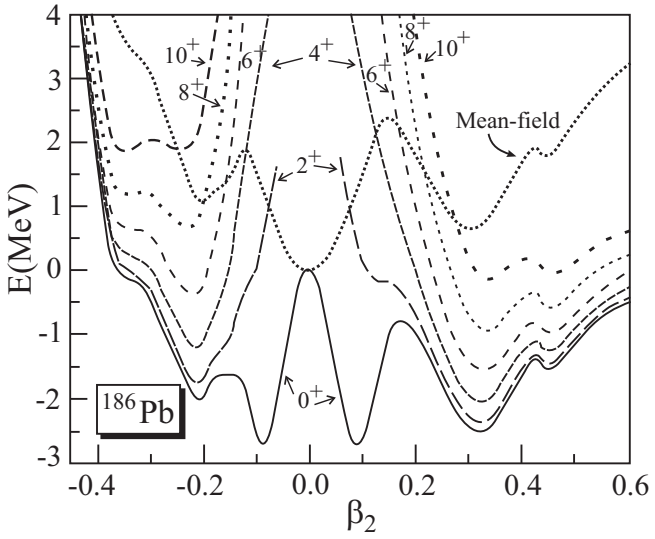

FIG. 19: Particle-number projected mean-field (small dotted curve and marked as 'Mean-field') as well as the particle- and angular-momentum projected energy curves (full, long-dashed,... lines), up to spin J=10 for ^{186}Pb, as a function of the quadrupole deformation variable β_2 (taken from [118]).

Inspecting Fig.19, one notices that for a given energy one cannot uniquely specify a given mean-field projected state. In order to obtain a genuine energy spectrum that can be

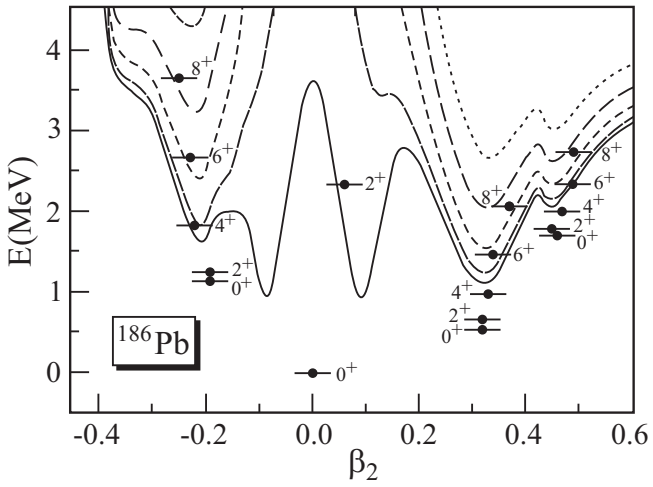

FIG. 20: Energy spectrum for the lowest-lying positive-parity bands in ^{186}Pb with even angular momentum J and K=0 as a function of the quadrupole deformation parameter, β_2. The particle- and angular-momentum energy curves are given as a reference. The excitation energy is derived from measuring the energy relative to the energy of the 0_1^+ ground state (taken from [118]).

compared with experimental data, one should go beyond the mean-field approach and diagonalize the Hamiltonian $\hat{H}$ in the space, $\{\mid JM;q\rangle\}$ of projected states. It is the parameter q which acts as a general collective coordinate that will generate the optimal superposition of projected mean-field states denoted as

$$\mid JM;k\rangle = \sum_q f_{J,k}(q) \mid JM;q\rangle, \tag{100}$$

where $f_{J,k}(q)$ are weight functions to be determined from the stationarity condition for the generator coordinate ground state (also called the GCM method, see Ch.10 in the book of Ring and Shuck [119])

$$\frac{\delta}{\delta f^*_{J,k}} . \frac{\langle JM;k \mid \hat{H} \mid JM;k\rangle}{\langle JM;k \mid JM;k\rangle} = 0. \tag{101}$$

This variational method leads to the Hill-Wheeler-Griffin equations [120, 121] that determine the eigenstates $\mid JM;k\rangle$ and corresponding energy eigenvalues $E_{J,k}$

$$\sum_{q'} [\langle JM;q \mid \hat{H} \mid JM;q'\rangle - E_{J,k}\langle JM;q \mid JM;q'\rangle] f_{J,k}(q') = 0. \tag{102}$$

For each value of J, the angular-momentum projected GCM method results in a correlated "ground state" and, in addition, a set of excited states from orthogonalization to the ground state (the weight functions $f_{J,k}(q)$ do not form an orthogonal set and are coherent states). The correct collective wave function can be expressed in the basis of the intrinsic states by the transformation $g_{J,k}(q) = \langle JM;k \mid JM;q\rangle$.

For the nucleus ^{186}Pb, discussed before in Fig. 19, the GCM method results in the energy spectrum shown in Fig. 20. In this figure, the projected energy curves are drawn again as a reference. This allows us to make an interesting presentation of the resulting energy spectrum, because the collective wave functions, $g_{J,k}(q)$, exhibit a given spread around the maximum probability. The bars represent the energies $E_{J,k}$ for each of the states, that are

plotted at the mean deformation, $\overline{q}_{J,k}$, in the intrinsic frame and are defined as

$$\overline{q}_{J,k} = \int g^2_{J,k}(q) q dq. \tag{103}$$

Thus, not only the energy spectrum (now normalized to the lowest $J^\pi=0^+$ state) can be seen, but at the same time interesting information about the value of the collective quadrupole parameter q is apparent.

Many calculations have been carried out during the last decades either starting from Skyrme forces (the recent studies make use of the SLy4 or SLy6 [122] for the particle-hole channel to which a density-dependent delta pairing for the particle-particle channel [123] has been added) or starting from the Gogny force. Recent studies using the Gogny force make use of the D1S parameterization [124, 125]. In view of the manifestation of shape coexistence throughout the nuclear mass surface, we present here the relevant references on this topic.. The references in the next two paragraphs use either Skyrme forces or the Gogny D1S interaction to calculate configuration mixing of angular-momentum and particle-number-projected mean-field states by means of the GCM.

Skyrme forces have been applied to the study of light nuclei starting from a HF + BCS approach for ^{24}Mg [126, 127], ^{32}S, ^{36}Ar, ^{38}Ar and ^{40}Ca [128], the neutron-deficient Kr nuclei [129] and the neutron-deficient Pb nuclei [118, 130–134].

The finite-range Gogny force has been used in particular by the Madrid group, using the HFB approach, studying light nuclei such as ^{30,32,34}Mg and ^{32,34,36,38}Si nuclei [135]. the N $\approx$ 20 nuclei [136], the N $\approx$ 28 nuclei [137], the Mg isotopes [138], a possible shell-closure at N=32 or 34 [139], nuclei in the Sn region [140, 141], a study of the rare-earth Nd nuclei [142], and also the neutron-deficient Pb nuclei [143–145].

More restricted self-consistent Skyrme Hartree-Fock plus BCS calculations have been carried out for the neutron-deficient Kr and Sr isotopes by Sarriguren [146] and for the neutron rich Yb, Hf, W, Os and Pt nuclei [147]. Calculations have been carried out for the Pd, Xe, Ba, Nd, Sm, Gd and Dy rare-earth nuclei, aiming to study the evolution of the minima characterizing the energy surfaces [148]. A very recent study of the energy surfaces covering the full triaxial landscape was carried out (see reference [149]) for the even-even Pt nuclei.

A different approach to study the dynamics of the full five-dimensional collective model (5DCH) results in the construction of a collective Bohr Hamiltonian in which the deformation dependence of the parameters (moments of inertia, mass parameters, energy of the zero-point motion) is determined from microscopic self-consistent mean-field studies. It has been shown that if the overlap of the mean-fields at different values of the collective coordinate q and q', i.e., $\mathcal{I}(q,q') \equiv \langle \Phi(q) \mid \Phi(q') \rangle$, is *approximated* by a Gaussian overlap (GOA), a Taylor expansion up to second order in the non-locality, $q-q'$, of the Hill-Wheeler equation gives rise to a collective Schrödinger equation [111, 119]. There has been quite some debate about which masses to be used: the GCM + GOA masses [150] or the ATDHF masses [151]. In most applications, the Inglis-Belyaev formula for the moments of inertia [152, 153] and the cranking approximation to calculate both the mass parameters associated with the β, γ coordinates and the zero-point energy correction associated with the rotational and vibrational kinetic energy [154] are used. As a consequence, these studies to solve the 5DCH can be regarded as a modern version of the model of Baranger and Kumar [155, 156].

Within this spirit, the Gogny force has been widely used solving the approximated 5DCH Schrödinger equation. The early calculations mainly concentrated on the collective potential for some rare-earth nuclei and nuclei in the Pb region [157, 158]. A more detailed study has been carried out for the ^{190,192,194}Hg nuclei by Delaroche *et al.* [159]. More recently, the full solution of the collective 5DCH has been studied within constrained HFB theory based on the Gogny D1S force. Studies in the Pb mass region have been carried out [160]; also

studying shell closure for light nuclei at N=16 [161] and for the N=20 and N=28 neutron-rich nuclei [162] and the role of triaxiality in the light Kr nuclei [163]. An extensive overview of low-lying collective properties over the whole mass region has been given, using the same methods, by Delaroche *et al.* [164].

A different approach was proposed by Walecka who developed a relativistic mean-field formulation (RMF)[165]. A detailed discussion on the Lagrangians used, is given in several review papers [166–169]. An interesting study within the relativistic Hartree-Bogoliubov (RHB) framework was performed specifically concentrating on shape coexistence in the Pt-Hg-Pb nuclei [170]. Within the RMF approach, beyond-relativistic-mean-field studies have been performed very recently, incorporating also configuration mixing of mean-field wave functions projected onto angular momentum J and particle number (N,Z), using the GCM approach, restricting to axially symmetric systems (encompassing vibrational and rotational degrees of freedom) with applications for ^{32}Mg and ^{194}Hg [171] (only J-projected) and for ^{24}Mg, ^{32}S and ^{36}Ar (J- and particle-number projected) [172]. Even more general studies have been performed using projected states starting from triaxial quadrupole constraints on the mean-field level with applications to the neutron-rich Mg nuclei [173] as well as using the resulting three-dimensional relativistic mean-field wave functions in a GCM configuration mixing calculation [174] with application for ^{24}Mg. We mention that more restricted studies of potential energy surfaces, aiming at the study of triaxial ground-state shapes for the Sm and Pt nuclei, making use of 3-dimensional RHB model have been performed [175] also.

Relativistic mean-field theory has also been used to extensively study the five-dimensional collective Hamiltonian (5DCH), starting from the relativistic energy density functional, and applied to the even-even Gd nuclei [176] and, more recently, to the study of even-even Ba and Xe nuclei [177].

VII. SIMILARITIES BETWEEN SHELL-MODEL AND MEAN-FIELD APPROACHES

We now come to the point that shell-model and mean-field approaches, if technically possible, lead to very much the same physics. It seems clear that starting from a spherical mean field only, and getting both the advantages and disadvantages from the ensuing spherical closed-shell configurations near stability, one inevitably runs out of computer capabilities. Moreover, the model wave functions do not give genuine physics insight (billions of components). Still, this approach is a consistent and robust approach with strong predictive power, such that systematic deviations between experiment and theory have to be taken seriously and cannot be hidden by parameter changes. On the other hand, making use of self-consistent mean-field methods, one starts from an effective nucleon-nucleon interaction in order to derive an optimized deformed (quadrupole deformation, pairing,..) basis $\mid \Phi(q)\rangle$. Whereas the shell-model space itself is a Hilbert space, the set of Slater determinants constitutes a geometrical surface within the Hilbert space (see reference [178] for a more detailed exposition of this point). The mean-field method produces an energy surface which is semi classical. As a consequence and in order to reach results to be compared with the data in nuclei, one needs to go beyond the mean-field approximation. Here, the technicalities of projecting from the intrinsic frame to the lab frame, with good J, N, Z,.. are very demanding when exploring the full space of the β, γ quadrupole variables. Moreover, one has to take into account mixing of the various intrinsic projected states in order to arrive at the exact eigenstates. Calculations starting from either a spherical shell-model basis, or, using mean-field methods (applied to the Mg-,S-, and Zr-istopes) resulted in a very strong resemblance (see reference [179] for a detailed discussion).

VIII. CONCLUSION

We have discussed the intertwinning of our understanding on nuclear forces and the low-lying nuclear structure properties. We started with on one side the rather crude description of the NN interaction, evolving into modern interactions describing nuclear scattering properties in great detail. On the other side, we have discussed important developments in the nuclear shell model, starting from an independent particle picture (IPM), adding the residual interaction allowing a description of nuclei with few particles outside of closed shells, moving to large model space with active protons and neutrons building up strongly correlated collective excitations (such as rotational motion). We have also discussed the phenomenological approach to collective excitations (vibrations, rotations,...) and discussed that self-consistent mean-field theory naturally leads to the appearance of deformed nuclear shapes. Going beyond the mean-field level, including nuclear dynamical effects, collective excitations appear in a natural way.

A particular important issue is understanding the effective in-medium interaction starting from our knowledge of the bare NN interaction.One can study the different routes (microscopic, phenomenological and schematic) and discuss the benefits and limitations of each of those methods. It is good to point out that recently (last decade), important steps have been taken to understand and construct the nucleon force in the atomic nucleus (including both 2- and 3-body forces) allowing to construct effective forces starting from chiral perturbation theory as a low-energy field theory consistent with the symmetries of QCD. This may result in a consistent approach to connect the observed nuclear properties with a genuine microscopic approach but would imply an extra couple of lectures on modern theories of nuclear forces which is outside the goals set out for the present lecture series.

IX. ACKNOWLEDGMENTS

The author (KH) thanks the FWO-Vlaanderen for financial support. These lecture notes form part of the training program within the framework of the BriX network (P7/12) funded by the "IUAP Programme - Belgian State - BSP".

---

[1] E. Rutherford, Phil. Mag. 21, 669 (1911)
[2] J. Chadwick, Proc. Roy. Soc. A136, 692 (1932)
[3] W. Heisenberg, Z. Phys. 77, 1 (1932)
[4] E. Wigner, Phys. Rev. 51, 106 (1937)
[5] E. Feenberg and M. Phillips, Phys. Rev. 51, 597 (1937)
[6] J. H. Bartlett, Phys.Rev. 49, 102 (1936)
[7] E. Majorana, Z. Phys. 82, 137 (1933)
[8] E. Fermi, E. Amaldi, O. D'Agostino, F. Rasetti and E. Segré, Proc. Roy. Soc. A146, 483 (1934)
[9] N. Bohr, Nature 137, 344 (1936)
[10] H. A. Bethe and R. F. Bacher, Revs. Mod. Phys. 8, 82 (1936)
[11] C. F. von Weizsäcker, Z. Phys. 96, 431 (1935)
[12] N. Bohr and J. A. Wheeler, Phys. Rev. 39, 426 (1939)
[13] Th. Schmidt, Z. Phys. 106, 358 (1937)
[14] H. Schüler and Th. Schmidt, Z. Phys. 96, 485 (1935)
[15] H. B. G. Casimir, On the Interaction Between Atomic Nuclei and Electrons, Prize Essay, Teyler's Tweede Genootschap, Haarlem, reprinted in 1963(123)

[16] C. H. Townes, H. M. Fowley and W. Low, Phys. Rev. 76, 1415 (1949)
[17] M. G. Mayer, Phys.Rev. 75, 1969 (1949)
[18] O. Haxel, J. H. D. Jensen and H. E. Suess, Phys. Rev. 75, 1766 (1949)
[19] A. Bohr, Mat. Fys. Med. Dan. Vid. Selsk 26, no14 (1952)
[20] A. Bohr and B. R. Mottelson, Mat. Fys. Med. Dan. Vid. Selsk. 27, no16 (1953)
[21] J. Rainwater, Phys.Rev. 79, 432 (1950)
[22] P.J.Brussaard and P.W.M.Glaudemans,*Shell-Model Applications in Nuclear Spectroscopy*, (North-Holland, Amsterdam, 1977).
[23] P. Ring and P.Schuck, *The Nuclear Many-Body Problem*, (Springer-Verlag, Berlin, 1980).
[24] H. Yukawa, Proc. Phys. Math. Soc. Japan, **17**, 48 (1935)
[25] A. Bohr and B.R. Mottelson,*Nuclear Structure: Volume I: Single-Particle Motion*, (Benjamin, New York, 1975).
[26] T.Hamada and I.Johnston, Nucl. Phys. **34**,382 (1962)
[27] T.Hamada, Y.Nakamura and R.Tamagaki, Progr. Theor. Phys. **33**,769 (1965)
[28] R.Reid Jr., Ann. Phys. (NY) **50**,411 (1968)
[29] F. Tabakin, Ann. Phys.(NY) 30, 51 (1964)
[30] M.Nagels, T.Rijhken and J. de Swart, Phys. Rev. D **17**,768 (1978)
[31] W.Cottingham *et al.*, Phys. Rev. D **8**,800 (1973)
[32] M.Lacombe *et al.*, Phys. Rev. C **21**,861 (1980)
[33] R.Machleidt, K.Holinde and C.Elster, Phys. Rep. **149**, 1 (1987)
[34] J.Haidenbauer and K.Holinde, Phys. Rev. C **40**, 2465 (1989)
[35] R.Machleidt, Phys. Rev. C **63**, 024001 (2001)
[36] V. G. J. Stoks, R. A. M. Klomp, C. P. F. Terheggen and J. J. de Swart, Phys. Rev. **C49**, 2950 (1994)
[37] B.Wiringa, R.Smith and T.Ainsworth, Phys. Rev. C **29**, 1207 (1984)
[38] B.Wirinaga, V.Stoks and R.Schiavilla, Phys. Rev. C **51**, 38 (1995)
[39] J.Carlson and R.Schiavilla, Rev. Mod. Phys. **70**, 743 (1998)
[40] V.Stoks and J.de Swart, Phys. Rev. C **47**, 761 (1993)
[41] S.Pieper, V.Pandharipandi, R.Wiringa and J.Carlson, Phys. Rev. C **64**, 014001 (2001)
[42] S.Pieper, Eur. Phys. J. A **13**, 75 (2002)
[43] S.Pieper, K.Varga and R.Wiringa, Phys. Rev. C **66**, 044310 (2002)
[44] R.Wiringa, I.Lin and S.Machida, Phys. Rev. Lett. **89**, 182501 (2002)
[45] N.Hoshizaki, I.Lin and S.Machida, Progr. Theor. Phys. **26**, 680 (1961)
[46] D.Wong, Nucl. Phys. **55**, 212 (1964)
[47] R.Bryan and B.Scott, Phys. Rev. **135**, B434 (1964)
[48] R.de Tourreil, B.Rouben and D.Sprung, Nucl. Phys. A **242**, 445 (1975)
[49] J.Côté, B.Rouben, R.de Tourreil and D.Sprung, Nucl. Phys. A **273**, 269 (1976)
[50] T.Obinata and M.Wada, Progr. Theor. Phys. **53**, 732 (1975)
[51] T.Obinata and M.Wada, Progr. Theor. Phys. **57**, 1984 (1977)
[52] T.Obinata and M.Wada, Progr. Theor. Phys. Progr. Lett. **73**, 1270 (1985)
[53] P.Povh, K.Rith, C.Scholz and F.Zetsche,*Particle and Nuclei: An Introduction to the Physical Concepts*, second,revised and enlarged ed. (Springer-Verlag, Berlin, 1999)
[54] E. Epelbaum, H.-W. Hammer and U. Meissner, Revs. Mod. Phys. **81**, 1773 (2009)
[55] S. E. Koonin, D. J. Dean and K. Langanke, Phys. Repts. **278**, 1 (1997)
[56] B. R. Barrett et al., Phys. Rev. **C66** (2002) 024314
[57] K. Heyde, *Basic Ideas and Concepts in Nuclear Physics,second edition*, (IOP Publishing, Bristol and Philadelphia, 1999)
[58] P. J. Nolan and P. J. Twin, Ann. Rev. Nucl. Part. Sci. **38** (1988) 533
[59] W. Heisenberg,Zeit. Phys. **77** (1932) 1
[60] E. P. Wigner, Phys. Rev. **51** (1937) 106
[61] M. G. Mayer, Phys. Rev. **75** (1949) 1968

[62] O. Haxel, J. H. D. Jensen and H. E. Suess, Phys. Rev. **75** (1949) 1766
[63] A. Bohr and B. Mottelson, *Nuclear Structure, vol.2*, (Benjamin, N. Y., 1975)
[64] J. P. Elliott, Proc. Roy. Soc. **A245** (1958) 128
[65] J. P. Elliott, Proc. Roy. Soc. **A245** (1958) 562
[66] K. Heyde, *The Nuclear Shell Model*, Springer-Verlag, Heidelberg, second and enlarged edition 2004
[67] E. Caurier, G. Martinez-Pinedo, F. Nowacki, A. Poves and A. P. Zuker, Revs. Mod. Phys. **77** (2005) 427
[68] K.Brueckner, Phys. Rev. **97**, 1353 (1955)
[69] H.Bethe and J.Goldstone, Proc. Roy. Soc.(London) A **238**, 551 (1957)
[70] J. Goldstone, Proc. Roy. Soc.**239**, 267 (1957)
[71] H. Bethe, B.H. Brandow and A. G. Petschek, Phys. Rev. **129**, 225 (1963)
[72] B. H. Brandow, Rev. Mod. Phys.**39**, 771 (1967)
[73] B.Day, Revs. Mod. Phys. **39**, 719 (1967)
[74] T.Kuo and G.Brown, Nucl. Phys. **85**, 40 (1966)
[75] T.Kuo and G.Brown, Nucl. Phys. **114**, 241 (1968)
[76] M. Hjorth-Jensen, T.Kuo and E.Osnes, Phys. Rep. **261**,125 (1995)
[77] G. Martinez-Pinedo, A. P. Zuker, A. Poves and E. Caurier, Phys. Rev.C55, 187 (1997)
[78] E.Pasquini and A.Zuker, in *Physics of Medium Light Nuclei, Florence, 1977*, ed. P.Blasi and R.Ricci (Editrici Compositrice, Bologna, 1978)
[79] A.Poves and A.Zuker, Phys. Rep. **70**, 235 (1981)
[80] F.Nowacki, Ph.D. Thesis, IReS, 1996
[81] A. Zuker, Phys. Rev. Lett. 90, 042502 (2003)
[82] S.Cohen and D.Kurath, Nucl. Phys. **73**, 1 (1965)
[83] P.Glaudemans, G.Wiechers and P.Brussaard, Nucl. Phys. **56**, 529 (1964)
[84] P.Glaudemans, G.Wiechers and P.Brussaard, Nucl. Phys. **56**, 548 (1964)
[85] B.Wildenthal, in *Varenna Lectures* **69**, 383 (1976)
[86] B.Wildenthal, in *Int.Symp. on Nuclear Shell Models*, ed. M.Valliérres and B.Wildenthal (World Scientific, Singapore,1976), p360
[87] A.Brown and B.Wildenthal, Ann. Rev. Nucl. Sci. **38**, 29 (1988)
[88] A. Brown and W. A. Richter, Phys. Rev. C **74**, 034315 (2006)
[89] M.Honma, T.Otsuka, A..Brown and T.Mizusaki, Phys. Rev. C **65**, 061301 (2002)
[90] M.Honma, T.Otsuka, A..Brown and T.Mizusaki, Phys. Rev. C **69**, 034335 (2004)
[91] M.Honma, T.Otsuka, A..Brown and T.Mizusaki, Eur. Phys. J. A **25, s01**, 499 (2006)
[92] A.Poves, J.Sánchez-Solano, E.Caurier and F.Nowacki, Nucl. Phys. A **694**, 157 (2001)
[93] M.Honma, T.Otsuka, T.Mizusaki and M. Hjorth-Jensen, Phys. Rev. C **80**, 064323 (2009)
[94] E. Caurier and F. Nowacki, Acta Phys. Pol. 30,705 (1999)
[95] B. A. Brown, A. Etchedgoyen, W. D. M. Rae, N. S. Godwin, W. A. Richter, C. H. Zimmerman, W. E. Ormand, and J. S. Winfield The computercode Oxbash, MSU-NSCL Report, No. 524, 1984
[96] T. Mizusaki, RIKEN Acc. Progr. Rept. 33, 14 (2000)
[97] B. A. Brown and W. D. M. Rae, NUSHELL@MSU MSU-NSCL Report 2007 (http://www.nscl.msu.edu/ brown/)
[98] http://www.fys.uio.no/compphys/cp/software.html
[99] E. W. Ormand and C. W. Johnson, Redstick code, 2002
[100] M. Valliéres and A. Novoselsky, Nucl. Phys. A570, 345c (1993)
[101] W.Richter, M.Van der Merwe, R.Julies and A.Brown, Nucl. Phys. A **523**, 325 (1991)
[102] L. Corragio, A. Covello, A. Gargano, N. Itaco and T.T. S. Kuo, Progr. Part. Nucl. Phys. 62, 135 (2009)
[103] E. Caurier, J. Menendez, F. Nowacki and A. Poves, Phys. Rev.C75, 054317 (2007)
[104] A. Zuker, J. Retamosa, A. Poves and E. Caurier, Phys. Rev.C53, 1741 (1995)

[105] A. Bohr, Mat. Fys. Med. Dan. Vid. Selsk. 26, No.14 (1952)
[106] A. Bohr and B. R. Mottelson, Mat. Fys. Med. Dan. Vid. Selsk. 27, No.16 (1953)
[107] J. Rainwater, Phys. Rev. 79, 432 (1950)
[108] A. Frank, J. Jolie and P. Van Isacker, *Symmetries in Atomic Nuclei: from Isospin to Supersymmetry*, Series: Springer Tracts in Modern Physics, vol. 230 (2009) (North-Holland, Amsterdam, 1977).
[109] D. Vautherin and D. M. Brink, Phys. Rev.C5, 626 (1972)
[110] D. Vautherin, Phys. Rev.C7, 296 (1973)
[111] M. Bender, H. Flocard and P.-H. Heenen, Phys. Rev. C68, 044321 (2003)
[112] T. H. R. Skyrme, Philos. Mag. 1, 1043 (1956)
[113] T. H. R. Skyrme, Nucl. Phys. 9, 615 (1959)
[114] T. H. R. Skyrme, Nucl. Phys. 9, 635 (1959)
[115] D. Gogny, in *Proceedings of the International Conference on Nuclear Physics*, ed. J. de Boer and H. J. Mang (North-Holland, Amsterdam, 1973), p. 48
[116] D. Gogny, in *Proceedings of the International Conference on Nuclear Self-Consistent Fields*, ed. G. Ripka and M. Porneuf (North-Holland, Amsterdam, 1975), p. 333
[117] J. Dechargé and D. Gogny, Phys. Rev. C21, 1568 (1980)
[118] T. Duguet, M. Bender, P. Bonche and P.-H. Heenen, Phys. Lett. B559, 201 (2003)
[119] P. Ring and P. Schuck , *The Nuclear Many-Body Problem* (Springer-Verlag, New-York, 1980)
[120] D. L. Hill and J. A. Wheeler, Phys. Rev. 89, 1102 (1953)
[121] J. J. Griffin and J. A. Wheeler, Phys. Rev. 108, 311 (1957)
[122] E. Chabanat, P. Bonche, P. Haensel, J. Meyer and R. Schaeffer, Nucl. Phys. A635, 231 (1998)
[123] C. Rigollet, P. Bonche, H. Flocard and P.-H. Heenen, Phys. Rev. C59, 3120 (1999)
[124] J.-F. Berger, M. Girod and D. Gogny, Nucl. Phys. A428, 23 (1984)
[125] J.-F. Berger, M. Girod and D. Gogny, Comput. Phys. Commun. 63, 365 (1991)
[126] A. Valor, P.-H. Heenen and P. Bonche, Nucl. Phys. A671, 145 (2000)
[127] M. Bender and P.-H. Heenen, Phys. Rev. C78, 024309 (2008)
[128] M. Bender, P.-H. Heenen and P.-G. Reinhard, Rev. Mod. Phys. 75, 121 (2003)
[129] M. Bender, P. Bonche and P.-H. Heenen, Phys. Rev. C74,024312 (2006)
[130] P.-H. Heenen, A. Valor, M. Bender, P. Bonche and H. Flocard, Eur. Phys. J. A11, 393 (2001)
[131] M. Bender, T. Cornelius, G. A. Lalazissis, J. A. Maruhn, W. Nazarewicz and P.-G. Reinhard, Eur. Phys. J. A14, 23 (2002)
[132] N. Smirnova, P.-H. Heenen and G. Neyens, Phys. Lett. B569, 151 (2003)
[133] M. Bender, P. Bonche, T. Duguet and P.-H. Heenen, Phys. Rev. C69, 064303 (2004)
[134] M. Bender and P.-H. Heenen, Eur. Phys. J. A25, 519 (2005)
[135] R. R. Rodríguez-Guzmán, J. L. Egido and L. M. Robledo, Phys. Lett. B474, 15 (2000)
[136] R. R. Rodríguez-Guzmán, J. L. Egido and L. M. Robledo, Phys. Rev. C62, 054319 (2000)
[137] R. R. Rodríguez-Guzmán, J. L. Egido and L. M. Robledo, Phys. Rev. C65, 024304 (2002)
[138] R. R. Rodríguez-Guzmán, J. L. Egido and L. M. Robledo, Nucl. Phys. A709, 201 (2002)
[139] T. R. Rodríguez-Guzmán and J. L. Egido, Phys. Rev. Lett. 99, 062501 (2007)
[140] T. R. Rodríguez-Guzmán, J. L. Egido and A. Jungclaus, Phys. Lett. B668, 410 (2008)
[141] M. Anguiano, J. L. Egido and L. M. Robledo, Phys. Lett. B545, 62 (2002)
[142] T. R. Rodríguez-Guzmán and J. L. Egido, Phys. Lett. B663, 49 (2008)
[143] R. R. Chasman, J. L. Egido and L. M. Robledo, Phys. Lett. B513, 325 (2001)
[144] J. L. Egido, L. M. Robledo and R. Rodríguez-Guzmán, Phys. Rev. Lett. 93, 082502 (2004)
[145] R. R. Rodríguez-Guzmán, J. L. Egido and L. M. Robledo, Phys. Rev. C69, 054319 (2004)
[146] P. Sarriguren, Phys. Rev. C79, 044315 (2009)
[147] P. Sarriguren, R. R. Rodríguez-Guzmán and L. M. Robledo, Phys. Rev. C77, 064322 (2008)
[148] L. M. Robledo, R. R. Rodríguez-Guzmán and P. Sarriguren, Phys. Rev. C78, 034314 (2008)
[149] R. R. Rodríguez-Guzmán, P. Sarriguren, L. M. Robledo and J. E. García-Ramos, Phys. Rev. C81, 024310 (2010)

[150] R. E. Peierls and J. Yoccoz, Proc. Roy. Soc. London Sect. A70, 381 (1957)
[151] D. J. Thouless and J. G. Valatin, Nucl. Phys. 31, 211 (1962)
[152] D. R. Inglis, Phys. Rev. 103, 1786 (1956)
[153] S. T. Belyaev, Nucl. Phys. 24, 322 (1961)
[154] M. Girod and B. Grammaticos, Nucl. Phys. A330, 40 (1979)
[155] M. Baranger and K. Kumar, Nucl. Phys. A110,490 (1969)
[156] K. Kumar, Nucl. Phys. A231, 189 (1978)
[157] M. Girod and P.-G. Reinhard, Phys. Lett. B117, 1 (1982)
[158] M. Girod, J. P. Delaroche, D. Gogny and J. F. Berger, Phys. Rev. Lett. 62,2452 (1989)
[159] J. P. Delaroche, M. Girod, J. Libert and I. Deloncle, Phys. lett. B232, 145 (1989)
[160] J. Libert, M. Girod and J. P. Delaroche, Phys. Rev. C60, 054301 (1999)
[161] A. Obertelli, S. Péru, J. P. Delaroche, A. Gillibert, M. Girod and H. Goutte, Phys. Rev. C71, 024304 (2005)
[162] S. Péru, M. Girod and J. F. Berger, Eur. Phys. J. A9,35 (200)
[163] M. Girod, J. P. Delaroche, A. Görgen and A. Obertelli, Phys. Lett. B676, 39 (2009)
[164] J. P. Delaroche, M. Girod, J. Libert, H. Goutte, S. Hilaire, S. Péru, N. Pillet and H. F. Bertsch, Phys. Rev. C81, 014303 (2010)
[165] J. D. Walecka, Ann. Phys. (N.Y.) 83, 491 (1974)
[166] B. D. Serot and J. D. Walecka, *Advances in Nuclear Physics*, (Plenum Press, New York, 1986), Vol. 16, p.1
[167] P.-G. Reinhard, Repts. Prog. Phys. 52, 439 (1992)
[168] B. D. Serot, Repts. Prog. Phys. 55, 1855 (1992)
[169] P. Ring, Prog. Part. Nucl. Phys. 37, 193 (1996)
[170] T. Nikšić, D. Vretenar, P. Ring and G. A. Lalazissis, Phys. Rev. C65, 054320 (2002)
[171] T. Nikšić, D. Vretenar and P. Ring, Phys. Rev. C73, 034308 (2006)
[172] T. Nikšić, D. Vretenar and P. Ring, Phys. Rev. C74, 064309 (2006)
[173] J. M. Yao, J. Meng, P. Ring and D. P. Arteaga, Phys. Rev. C79, 044312 (2009)
[174] J. M. Yao, J. Meng, P. Ring and D. Vretenar, Phys. Rev. C81, 044311 (2010)
[175] T. Nikšić, P. Ring, D. Vretenar, Y. Tian and Z.-y Ma, Phys. Rev. C81, 054318 (2010)
[176] T. Nikšić, Z. P. Li, D. Vretenar, L. Próchniak, J. Meng and P. Ring, Phys. Rev. C79, 034303 (2009)
[177] Z. P. Li, T. Nikšić, D. Vretenar and J. Meng, Phys. Rev. C81, 034316 (2010)
[178] D. J. Rowe and J. L. Wood, *Fundamentals of Nuclear Models Foundational Models*, (World Scientific, Singapore, 2010)
[179] P.-G. Reinhard, D. J. Dean, W. Nazarewicz, J. Dobaczewski, J. A. Maruhn and M. R. Strayer, Phys. Rev. 60, 014316 (1999)